





GABA is a modulator, rather than a classical transmitter, in the medial nucleus of the trapezoid body–lateral superior olive sound localization circuit

Alexander U. Fischer¹ , Nicolas I. C. Müller¹ , Thomas Deller², Domenico Del Turco², Jonas O. Fisch¹, Désirée Griesemer¹ , Kathrin Kattler³, Ayse Maraslioglu¹, Vera Roemer¹, Matthew A. Xu-Friedman⁴, Jörn Walter³ and Eckhard Friauf¹ 

¹Animal Physiology Group, Department of Biology, University of Kaiserslautern, D-67663, Kaiserslautern, Germany

²Institute of Clinical Neuroanatomy, Neuroscience Center, Goethe-University Frankfurt, Theodor-Stern-Kai 7, D-60590, Frankfurt am Main, Germany

³Genetics/Epigenetic Group, Department of Biological Sciences, Saarland University, D-66123, Saarbrücken

⁴Department of Biological Sciences, University at Buffalo, State University of New York, Buffalo, NY 14260, USA

Edited by: Ian Forsythe & Maike Glitsch

Key points

- The lateral superior olive (LSO), a brainstem hub involved in sound localization, integrates excitatory and inhibitory inputs from the ipsilateral and the contralateral ear, respectively. In gerbils and rats, inhibition to the LSO reportedly shifts from GABAergic to glycinergic within the first three postnatal weeks.
- Surprisingly, we found no evidence for synaptic GABA signalling during this time window in mouse LSO principal neurons. However, we found that presynaptic GABA_BRs modulate Ca²⁺ influx into medial nucleus of the trapezoid body axon terminals, resulting in reduced synaptic strength. Moreover, GABA elicited strong responses in LSO neurons that were mediated by extrasynaptic GABA_ARs. RNA sequencing revealed highly abundant δ subunits, which are characteristic of extrasynaptic receptors.
- Whereas GABA increased the excitability of neonatal LSO neurons, it reduced the excitability around hearing onset.
- Collectively, GABA appears to control the excitability of mouse LSO neurons via extrasynaptic and presynaptic signalling. Thus, GABA acts as a modulator, rather than as a classical transmitter.

Abstract GABA and glycine mediate fast inhibitory neurotransmission and are coreleased at several synapse types. Here we assessed the contribution of GABA and glycine in synaptic transmission between the medial nucleus of the trapezoid body (MNTB) and the lateral superior

Alexander Fischer received his PhD in Biology at the University of Kaiserslautern, where he worked on fast synaptic transmission in the auditory system, with special interest in short-term plasticity of inhibitory synapses. He recently headed to industry and follows his interest in deep analysis of data in the area of natural language understanding, utilizing principals of artificial intelligence. **Nicolas Müller** received an MSc in Cell and Neurobiology and is currently finishing his PhD thesis in the lab of Eckhard Friauf (University of Kaiserslautern). In his thesis, he studied synaptic elimination and strengthening of the MNTB–LSO projection upon peripheral and central manipulations of the auditory system. By doing so, he gained mechanistic insight in the elimination and strengthening process.



A. Fischer and N. Müller contributed equally to this work.

olive (LSO), two nuclei involved in sound localization. Whole-cell patch-clamp experiments in acute mouse brainstem slices at postnatal days (P) 4 and 11 during pharmacological blockade of GABA_A receptors (GABA_ARs) and/or glycine receptors demonstrated no GABAergic synaptic component on LSO principal neurons. A GABAergic component was absent in evoked inhibitory postsynaptic currents and miniature events. Coimmunofluorescence experiments revealed no codistribution of the presynaptic GABAergic marker GAD65/67 with gephyrin, a postsynaptic marker for GABA_ARs, corroborating the conclusion that GABA does not act synaptically in the mouse LSO. Imaging experiments revealed reduced Ca²⁺ influx into MNTB axon terminals following activation of presynaptic GABA_BRs. GABA_BR activation reduced the synaptic strength at P4 and P11. GABA appears to act on extrasynaptic GABA_ARs as demonstrated by application of 4,5,6,7-tetrahydroisoxazolo[5,4-c]pyridin-3-ol, a δ -subunit-specific GABA_AR agonist. RNA sequencing showed high mRNA levels for the δ -subunit in the LSO. Moreover, GABA transporters GAT-1 and GAT-3 appear to control extracellular GABA. Finally, we show an age-dependent effect of GABA on the excitability of LSO neurons. Whereas tonic GABA increased the excitability at P4, leading to spike facilitation, it decreased the excitability at P11 via shunting inhibition through extrasynaptic GABA_ARs. Taken together, we demonstrate a modulatory role of GABA in the murine LSO, rather than a function as a classical synaptic transmitter.

(Resubmitted 21 December 2018; accepted after revision 18 February 2019; first published online 18 February 2019)

Corresponding author E. Friauf: Animal Physiology Group, Department of Biology, University of Kaiserslautern, Kaiserslautern, Germany. Email: eckhard.friauf@bio.uni-kl.de

Introduction

Fast-acting inhibitory neurotransmission in the vertebrate central nervous system is mainly achieved by glycine and γ -aminobutyric acid (GABA). Glycine acts via ligand-gated Cl⁻ channels (GlyRs) comprising only two classes of subunits (α and β), its action thus being of a relatively uniform nature (Lynch, 2004, 2009; Betz & Laube, 2006). Metabotropic glycine receptors have not been identified in mammals (Tritsch *et al.* 2016). By contrast, GABAergic signalling appears to be much more complex, because it is mediated through heteropentameric ionotropic receptors (GABA_{A/C}Rs) composed of eight classes of subunits (α , β , γ , δ , ϵ , θ , π , ρ) with a total of 19 identified isoforms (Rudolph & Möhler, 2014; Smart, 2015; Naffaa *et al.* 2017). Moreover, GABA can act on G protein-coupled receptors (GABA_BRs), which are also very heterogeneous, displaying pronounced diversity in subcellular location, functional properties and cellular signalling (Brenowitz *et al.* 1998; Xu *et al.* 2014; Schwenk *et al.* 2016). Apart from targeting GABA_{A/C}Rs and GABA_BRs in sub- and presynaptic regions, GABA can escape the synaptic cleft and bind to extrasynaptic receptors, thus exerting tonic effects via a non-synaptic path (Otis *et al.* 1991; Barbour & Häusser, 1997; Farrant & Nusser, 2005; Lee & Maguire, 2014). Finally, GABA may be released not only from GABAergic neurons, but also from astrocytes, thereby operating as a gliotransmitter (Yoon & Lee, 2014; Gundersen *et al.* 2015).

GABA and GABA_ARs are widely distributed in the CNS. By contrast, glycine is of greater importance in the brainstem and spinal cord (Smart & Paoletti, 2012). In several

neural systems, glycine and GABA coexist in presynaptic axon terminals and in synaptic vesicles from which they can be released together (Ottersen *et al.* 1988; Todd *et al.* 1996; Jonas *et al.* 1998; O'Brien & Berger, 1999; Keller *et al.* 2001; Dugué *et al.* 2005; Crook *et al.* 2006; Dufour *et al.* 2010; Hirtz *et al.* 2012; Rahman *et al.* 2013; Nerlich *et al.* 2014; Ramakrishnan *et al.* 2014; Vaaga *et al.* 2014; Moore & Trussell, 2017). Therefore, mixed GABA–glycine inhibition has been implicated (Kotak *et al.* 1998; Dumoulin *et al.* 2001; Keller *et al.* 2001; Muller *et al.* 2006; Dufour *et al.* 2010; Apostolides & Trussell, 2013; Ishibashi *et al.* 2013; Nerlich *et al.* 2017; but see Hnasko & Edwards, 2012).

In the present study, we analysed GABAergic effects at fast inhibitory synapses in the auditory brainstem of mice. In mature animals, these synapses are glycinergic (Casparly & Finlayson, 1991) and tuned for resilience, reliability and temporal precision, even under sustained activation at stimulation frequencies >100 Hz (Kramer *et al.* 2014; Krächan *et al.* 2017). They connect the medial nucleus of the trapezoid body (MNTB) with the lateral superior olive (LSO) and form a crucial link in sound localization based on detecting interaural level differences (for a review, see Grothe & Pecka, 2014). Our analysis involved patch-clamp recordings, pharmacology, coimmunolabelling, calcium imaging and RNA sequencing. We obtained no evidence for functional GABAergic synapses in the LSO or a shift from GABAergic to glycinergic neurotransmission, unlike findings in gerbils and rats (Kotak *et al.* 1998; Nabekura *et al.* 2004). Instead, our results point towards postsynaptic GABA effects at extrasynaptic GABA_ARs throughout

development, mediating tonic activity rather than phasic inhibition. GABA also acts at MNTB axon terminals. Based on our results, it appears that ambient GABA modulates the excitability of LSO neurons. During the first postnatal week, when the internal Cl^- concentration $[\text{Cl}^-]_i$ is high and Cl^- flux leads to depolarization (Kandler & Friauf, 1995; Ehrlich *et al.* 1999; Löhre *et al.* 2005), GABA appears to increase the excitability. The opposite effect, namely suppression of excitation, occurs later in development, at times when Cl^- flux leads to hyperpolarization. We conclude that GABA acts in concert with glycine at MNTB–LSO synapses in an activity-dependent fashion and exerts a modulatory function, thus allowing fine-tuning of the magnitude and duration of fast and phasic synaptic inhibition (Tritsch *et al.* 2016).

Methods

Ethical approval

Experiments were approved by the regional council according to the German Animal Protection Law (TSchG §4, Absatz 3) and followed the NIH *Guide for the Care and Use of Laboratory Animals*. Moreover, the authors understand, and the work conforms to, the principles and regulations of *The Journal of Physiology* (Grundy, 2015).

Animals

Most experiments were performed on C57BL/6N mice of both sexes that were raised in the animal facilities of the University of Kaiserslautern or purchased from Charles River (Sulzfeld, Germany). Animals were housed on a 12 h light–dark cycle with *ad libitum* access to food and water. The day of birth was designated as postnatal day (P) 0. Calcium imaging experiments were performed at the State University of New York at Buffalo on CBA/CaJ mice of both sexes which were raised in the local animal facilities. Analysis was done at $\text{P}4 \pm 1$, $\text{P}11 \pm 1$, or $\text{P}60$.

Electrophysiology

After decapitation, mouse brains were quickly removed from the skull and transferred into ice-cold preparation solution, containing (in mM): 2.5 KCl, 1 MgCl_2 , 1.25 NaH_2PO_4 , 2 sodium pyruvate, 3 *myo*-inositol, 26 NaHCO_3 , 260 D-glucose, 2 CaCl_2 (pH 7.4, when bubbled with carbogen; 325 ± 10 mosmol/L). Coronal slices of 270 μm thickness were cut on a VT1200 S vibrating blade microtome (Leica Microsystems, Wetzlar, Germany). For recovery, they were incubated at 37°C for 55 min in artificial cerebral spinal fluid (ACSF) containing (in mM): 125 NaCl, 2.5 KCl, 1 MgCl_2 , 1.25 NaH_2PO_4 , 2 sodium pyruvate, 3 *myo*-inositol, 0.44 L-ascorbic acid,

25 NaHCO_3 , 10 D-glucose, 2 CaCl_2 (pH 7.4, when bubbled with carbogen; 295 ± 5 mosmol/L). After another 0.5–8 h at room temperature, slices were transferred into the recording chamber. Whole-cell patch-clamp recordings ($V_{\text{hold}} = -70$ mV) were performed with an Axioscope 2 FS microscope (Zeiss; Carl Zeiss Microscopy, Jena, Germany) or an Eclipse E600N (Nikon, Tokyo, Japan) both equipped with IR-DIC optics (Zeiss Fluor $\times 5/0.25 \infty/0.17$; Olympus LUMPlanFL N $\times 60/1.00 \text{ W} \infty/0/\text{FN}26.5$ (Olympus, Tokyo, Japan); Nikon $\times 4$ CFI Achromat, 0.1 ∞ ; $\times 60$ CFI Fluor W, 1.00 $\text{W} \infty$). Slices were continuously superfused with ACSF (1–2 ml/min, 22–27°C or $36 \pm 1^\circ\text{C}$) and visualized with an Orca-05G (Hamamatsu, Hamamatsu city, Japan) or a VX 44 (PCO computer optics) CCD camera. Principal LSO neurons were identified by their spindle-shaped somata and electrophysiological properties (Sternborg *et al.* 2010). Patch pipettes were pulled from glass capillaries (Science Products, Hofheim am Taunus, Germany) with a P-87 horizontal puller (Sutter Instrument Co., Novato, CA, USA). Pipette resistances ranged from 3 to 6 M Ω when filled with internal solution containing (in mM): 140 potassium gluconate, 10 HEPES, 5 EGTA, 1 MgCl_2 , 2 Na_2ATP , 0.3 Na_2GTP (280 ± 10 mOsm/L). The liquid junction potential of 15.4 mV was corrected online. This internal solution was used for some P4 recordings (Figs 1, 2 and 8A) and most P11 recordings (Figs 1, 2, 5, 7, 8A, 10 and 11). Another set of P4 recordings (Figs 5, 7 and 12) was performed with a near-physiological internal chloride concentration for this age, which contained (in mM): 110 potassium gluconate, 30 KCl, 10 HEPES, 5 EGTA, 1 MgCl_2 , 2 Na_2ATP , 0.3 Na_2GTP (285 ± 10 mOsm/L). In a subset of experiments (Figs 3 and 8B) the chloride driving force was increased by using an internal solution with a high chloride concentration containing (in mM): 130 KCl, 10 HEPES, 5 EGTA, 1 MgCl_2 , 2 Na_2ATP , 0.3 Na_2GTP (280 ± 10 mOsm/L; uncorrected liquid junction potential of -3.5 mV). Recordings were obtained with an EPC9 or EPC10 amplifier and PatchMaster software (HEKA Elektronik, Lambrecht (Pfalz), Germany). Recordings were discarded if the series resistance R_s changed $>20\%$. The membrane resistance was determined as $R_M = R_{\text{in}} - R_s$, with R_{in} representing the input resistance. R_s and R_{in} were derived from partially compensated current traces during 1 Hz triplets of -5 mV voltage steps (Fig. 11Bb).

For focal electrical stimulation of MNTB input fibres, TST150 theta electrodes (WPI, Sarasota, FL, USA) or patch pipette with tip diameters of ~ 20 and ~ 5 μm , respectively, were filled with ACSF, connected to a STG4004 (Multichannel Systems, Reutlingen, Germany) or Master8/Isoplex stimulator (A.M.P.I., Jerusalem, Israel) and placed at the lateral edge of the ipsilateral MNTB. Bipolar or monopolar rectangular current pulses (100–200 μs) of 20–16,000 μA intensity were applied

at 0.2–1 Hz, evoking inhibitory postsynaptic currents (eIPSCs) of short latencies (P4: 2–5 ms; P11: 1–3 ms). In some experiments, 3 μM CGP55845 was bath-applied to prevent GABA_BR activation. GlyRs and GABA_ARs were blocked with 100 nM strychnine and 10 μM GABAzine (GBZ alias SR95531), respectively.

Transmitters (100 μM GABA or 100 μM glycine) or agonists (1 μM 4,5,6,7-tetrahydroisoxazolo[5,4-c]pyridin-3-ol (THIP; alias gaboxadol or OV101) or 10 μM baclofen) were puff-applied 10–20 μm distant from patched somata via theta electrodes (TST150, WPI) or patch electrodes (tip diameters: \sim 2–5 μm). To do so, puffs (5–10 psi) were generated with a Multi-channel Picospritzer (Science Products) or a PDES-02DX (NPI Electronic, Tamm, Germany). In some experiments, 10 μM NO-711, a specific GAT-1 blocker, or 40 μM SNAP-5114, a specific GAT-3 blocker, were bath applied (in the following denoted as NO and SNAP, respectively). To avoid ‘washout’ of bath-applied blockers by puffing GABA_AR agonists, the second channel of the theta electrode was filled with the agonist plus the blocker. In order to address possible changes in action potential generation due to tonic GABAergic inhibition, GABA (1–100 μM) was puff-applied for 10 s, starting 5 s prior to depolarizing current injections (see Fig. 11Aa). Tonic inhibition was achieved within 3–5 s, when the GABA-induced hyperpolarization had reached a steady state. When steady-state depolarization was not reached early enough, puff application was prolonged to 15 s.

Glutamatergic events were blocked with 5 mM kynurenic acid or 20 μM CNQX. Miniature IPSCs (mIPSCs) were isolated with 1 μM tetrodotoxin (TTX). Glycinergic or GABAergic mIPSCs were identified in the presence of bath-applied 10 μM GBZ or 1 μM strychnine, respectively. In one series of experiments, mIPSCs were recorded from LSO or inferior colliculus neurons with the GABA_AR modulator pentobarbital (30 μM) in the bath. mIPSCs were analysed with MiniAnalysis 6.0.3 (Synaptosoft, Fort Lee, NJ, USA) when their decay phase could be fitted with an $R^2 > 0.85$. mIPSC decay times under pentobarbital were determined as follows. Because of the possibility of mixed transmitters, we did not assume a single exponential decay for the mIPSCs in pentobarbital. Instead, the decay course was fitted to a double-exponential function:

$$f(t) = A_1 \times e\left(-\frac{t}{\tau_1}\right) + A_2 \times e\left(-\frac{t}{\tau_2}\right),$$

where t is time, A_1 and A_2 are the peak amplitudes of the fast and the slow decay components at $t = 0$, and τ_1 and τ_2 are fast and slow decay time constants, respectively. From this, we calculated the weighted decay time constant τ_w :

$$\tau_w = \frac{A_1 \times \tau_1}{A_1 + A_2} + \frac{A_2 \times \tau_2}{A_1 + A_2}.$$

Files were analysed using IGOR Pro 6.3 (Wavemetrics, Lake Oswego, OR, USA), running Patcher’s Power Tools (Max Planck-Institute for Membrane Biophysics) with customized routines.

Calcium imaging

Brainstem slices were prepared and stored as described above. The preparation solution contained (in mM): 76 NaCl, 25 NaHCO₃, 75 sucrose, 25 glucose, 2.5 KCl, 1.25 NaH₂PO₄, 7 MgCl₂, 0.5 CaCl₂; and the ACSF contained (in mM): 125 NaCl, 26 NaHCO₃, 1.25 NaH₂PO₄, 2.5 KCl, 1 MgCl₂, 1.5 CaCl₂, 20 glucose, 4 sodium L-lactate, 2 sodium pyruvate, 0.4 sodium L-ascorbate. MNTB somata/axons were loaded using a borosilicate pipette (5–8 μm tip diameter) filled with ACSF, containing 0.05% fast-green (Sigma-Aldrich, St. Louis, MO, USA) and 110 μM magnesium-green (Mg-green, M3735, Thermo Fisher Scientific, Carlsbad, CA, USA). Axonal uptake of the dye was achieved by continuous pressure application at the dorsolateral edge of the MNTB for 30–45 min. A second pipette with a tip diameter of 20–30 μm was placed at the ventrolateral edge of the MNTB to immediately suck away excess dye (Regehr & Atluri, 1995). After loading, slices were stored in ACSF at room temperature for at least 1 h to allow diffusion of the dye along the axons. Electrical stimulation was performed as described above. Calcium signals were visualized with a $\times 60$ objective attached to an Olympus BX51WI microscope equipped with a 150 W xenon light source (Optiquip Model 770; OPTIQUIP, Rochester, UK) and a FITC U-N41001 (Olympus) filter set. Recordings with a Sensicam QE (Cooke Corp., Auburn Hills, MI, USA) at 2×2 binning allowed a spatial resolution of $\sim 0.1 \mu\text{m}/\text{pixel}$. For identification of loaded presynaptic terminals, a 7–9 px Gaussian filter was utilized in a test stimulation prior to the actual experiment. High temporal resolution recordings at 5 kHz were performed with a custom-made single photodiode system (Hamamatsu S1336-BK) connected to a BNC-2090 interface (National Instruments, Austin, TX, USA). To improve the signal to noise ratio of the photodiode, the field of view was constrained to 40–70 μm with a diaphragm and 30 traces were averaged (20 s interstimulus intervals). Camera settings, shutter and stimulation timings, data acquisition as well as analysis were performed with IGOR Pro 6.2 (Wavemetrics), running SIDX drivers (Bruxton Corp., Seattle, WA, USA), and custom software (mafPC).

Immunohistochemistry

Deeply anaesthetized mice (7% chloral hydrate, 0.01 ml/g body weight, i.p.) were transcardially perfused with 15 mM phosphate-buffered saline (PBS; pH 7.4, room temperature), followed by ice-cold 4% paraformaldehyde

for 20 min (Ecoline VC-360 pump, IsmaTec, Wertheim, Germany). Brains were removed from the skull, postfixed for 2 h in 4% paraformaldehyde, and stored overnight in 30% sucrose–PBS. Coronal brainstem slices were cut at 40 μm with a sliding microtome (HM 430, Thermo Fisher Scientific) and transferred into 15% sucrose–PBS for 5 min; 3 \times 10 min rinse steps in PBS followed at room temperature. Antibodies against gephyrin (1:500, host: mouse, Synaptic Systems, Göttingen, Germany), GlyT2 (1:10,000, host: guinea pig, Chemicon, Limburg an der Lahn, Germany) and GAD65/67 (1:1,000, host: rabbit, Abcam, Cambridge, UK) were applied free-floating at 4°C overnight in blocking solution (0.3% Triton X-100, 5% goat serum, 1% BSA in PBS), followed by rinsing 3 \times 10 min in PBS at room temperature. Slices were then incubated in the dark for 2 h in blocking solution and secondary antibody (1:1000; goat-anti-mouse, Alexa Fluor 647, Thermo Fisher Scientific; goat-anti-guinea pig, Alexa Fluor 488, Thermo Fisher Scientific; goat-anti-rabbit, Alexa Fluor 488, Thermo Fisher Scientific) and rinsed 3 \times 10 min in PBS. Cell nuclei were stained with propidium iodide (1 $\mu\text{g}/\text{ml}$ in PBS, Sigma-Aldrich) for 10 min and slices were rinsed again 3 \times 10 min in PBS. Slices were then mounted on gelatin-coated glass slides and covered with mounting medium containing 2.5% 1,4-diazabicyclo[2.2.2]octane (DABCO; Sigma-Aldrich).

Images were acquired with a confocal microscope equipped with an EC Plan-Neofluar \times 40/1.3 oil objective (LSM700, Zeiss). Intensity profiles across inhibitory synapses were determined in ZEN2012 (blue edition, Zeiss) by scan lines, drawn from the centre of the cell soma across membrane-associated gephyrin signals (see Fig. 4A). We analysed 7–18 and 1–3 intensity profiles per cell at P11 and P4, respectively. The position of maximal gephyrin signal was set to zero; negative and positive scan positions indicate intracellular and extracellular location, respectively. Prior to codistribution analysis (Bolte & Cordelières, 2006), a rolling ball background subtraction (radius 20) was applied with Fiji ImageJ 1.48 (Schindelin *et al.* 2012), followed by brightness adjustment. Regions of interest (ROIs) outreached the cell somata by 1–2 μm , and Pearson's coefficient, together with the corresponding Costes P -value (P_{Costes} , 200 repetitions), was determined with the Fiji plugin Coloc2. Codistribution became significant with $P_{\text{Costes}} \geq 0.95$.

RNA sequencing

Coronal brainstem cryosections of 30 μm thickness from P60 mice were placed on PEN membrane glass slides (Leica Microsystems) and dehydrated twice in ascending ethanol (75%, 95%, 100%, 1 min each). LSO tissue was collected using an LMD6500/DM6000B laser microdissection system (Leica Microsystems). For RNA extraction, we used an Arcturus PicoPure RNA Isolation

Kit (Thermo Fisher Scientific). RNA quality control and cDNA synthesis were done as described earlier (Picelli *et al.* 2013). Libraries were prepared with the Nextera DNA Library Preparation Kit (Illumina, Inc., San Diego, CA, USA) and sequenced 1 \times 100 bp on a HiSeq 2500 (Illumina). Reads were trimmed for adapter sequences and low quality (phred score < 20) with Trim Galore! (v0.4.2; http://www.bioinformatics.babraham.ac.uk/projects/trim_galore), aligned to the mm10 mouse reference genome using two-step STAR (v2.5.2a) alignment (Dobin & Gingeras, 2015) and marked for PCR duplicates with Picard tools (MarkDuplicate v1.115; <http://broad-institute.github.io/picard/>). Gene-wise read counts were summarized with featureCounts (Liao *et al.* 2014) using Gencode annotation vM2 and normalized as counts per million (CPM) to set a threshold for expressed genes (CPM ≥ 0.5), and as reads per kilobase per million (RPKM) to compare expression levels.

Statistics

Statistical analysis was performed with the Microsoft Excel plugin Winstat 2012.1 (R. Fitch Software). Gaussian distributed (Kolmogorov–Smirnov test) samples were compared in paired or unpaired two-tailed Student's t test, and a Wilcoxon signed rank test or a Mann–Whitney U test was applied otherwise. Equality of variances in unpaired t tests was determined with F test, and a homo- or heteroskedastic test was performed when appropriate. Bar charts are presented as the mean \pm SEM with single data points depicted by dots (connected if paired). Significance levels are indicated as follows: $P < 0.05$ *, $P < 0.01$ **, $P < 0.001$ ***; no symbols if $P > 0.05$. In Figs 8Bc and 10Cb, critical α values were *post hoc* Šidák corrected (Abdi, 2007).

Results

No GABA contribution to synaptic transmission at mouse MNTB–LSO inputs

In order to assess the transmitter phenotype of MNTB–LSO synapses in immature mice, we performed whole-cell recordings from LSO neurons at P4 and P11 while electrically stimulating MNTB fibres (Fig. 1Aa and b). Averaged eIPSC amplitudes in response to 1 Hz stimulation were robust over time (Fig. 1Ac) and revealed an \sim 5-fold amplitude increase between P4 and P11 (Fig. 1Ba–d; P4: 46 ± 8 pA, $n = 8$; P11: 236 ± 67 pA, $n = 9$; $P = 0.022$, unpaired t test). Likewise, decay kinetics accelerated 3.3-fold with age (Fig. 1Ca and b; P4: 22.1 ± 2.9 ms, $n = 8$; P11: 6.7 ± 1.5 ms, $n = 7$; $P = 6.3 \times 10^{-4}$, unpaired t test). GABAergic and glycinergic inputs were pharmacologically separated at the putatively mixed MNTB–LSO synapses (Fig. 1Ad).

Wash-in of the GlyR antagonist strychnine (100 nM) blocked eIPSCs by $74 \pm 4\%$ at P4 and by $88 \pm 4\%$ at P11, demonstrating a very prominent glycinergic component at both ages (Fig. 1*Ba–e*; P4: $n = 8$, $P = 5.9 \times 10^{-7}$; P11: $n = 9$, $P = 1.0 \times 10^{-8}$; paired *t* tests). At 100 nM, strychnine is insufficient to completely block GlyRs, but non-specific inhibition of GABA_ARs is avoided (Jonas *et al.* 1998; see

also Fig. 2*B*). Thus, we most likely underestimated the prominent glycinergic component. Additional wash-in of the high-affinity GABA_AR antagonist GBZ (10 μ M; $K_d = 0.15 \mu$ M) further reduced eIPSC amplitudes only slightly by $12 \pm 3\%$ at P4 and by as little as $4 \pm 1\%$ at P11 (Fig. 1*Ba–e*; P4: $n = 8$, $P = 0.009$; P11: $n = 7$, $P = 0.016$; paired *t* tests). When normalized to

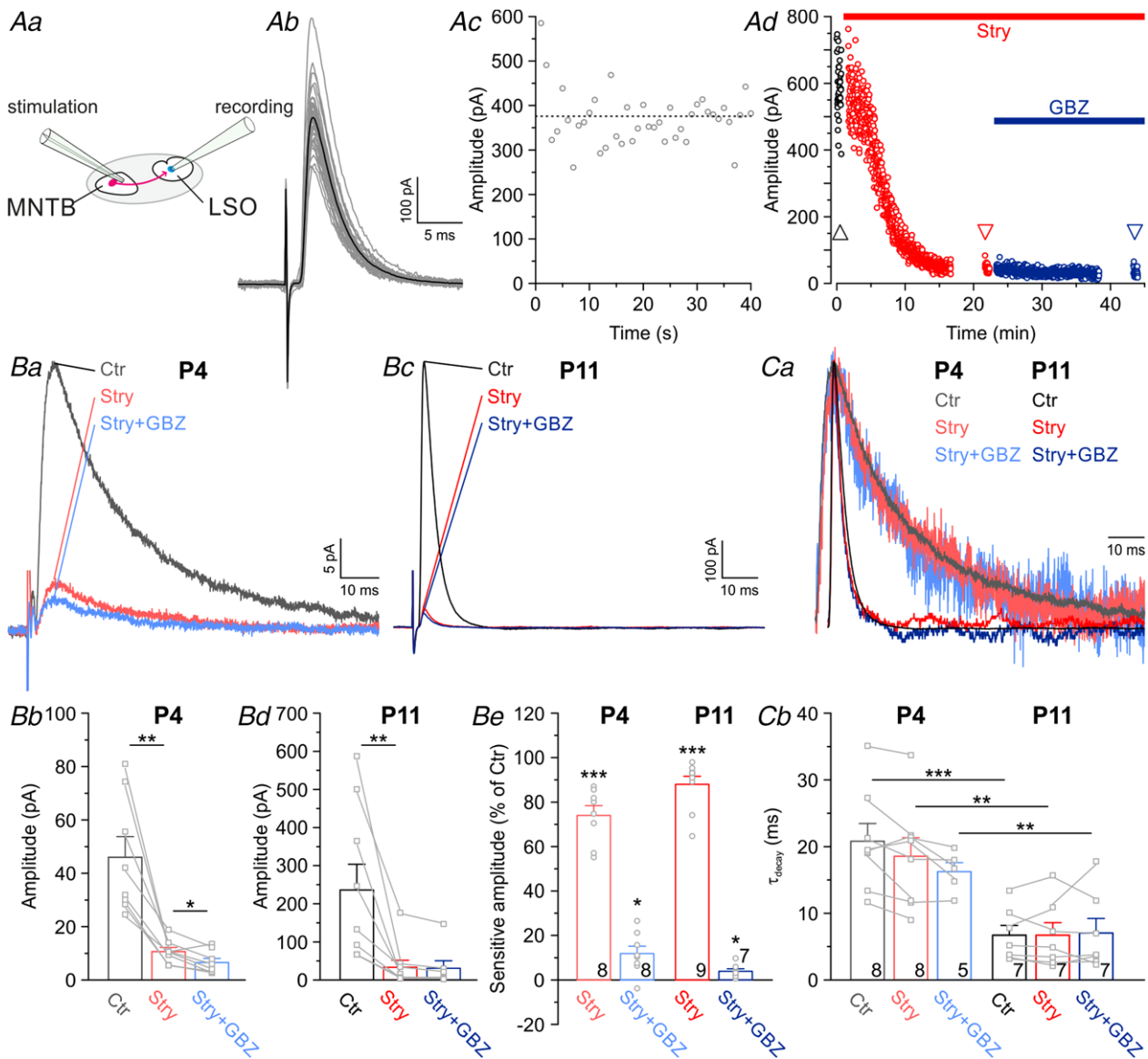


Figure 1. Synaptic transmission at mouse MNTB–LSO inputs is mediated by glycine, not by GABA

Aa, MNTB–LSO synapses were activated at 1 Hz by focal electrical stimulation of MNTB axons. Ab and c, evoked IPSCs (eIPSCs) at P11, demonstrating their robustness and stability. Grey traces represent overlays of 40 repetitive events, with the average in black. Dashed line in Ac marks mean peak amplitude. Ad, pharmacological characterization of a P11 LSO neuron. Subsequent blockade of glycine receptors (GlyRs) with strychnine (100 nM Stry) and GABA_A receptors (GABA_ARs) with GABA_Azine (10 μ M GBZ) abolished eIPSCs nearly completely. Ba and c, eIPSCs at P4 and P11, revealing a large glycinergic component, yet a virtually absent GABAergic component. Traces in Bc are from the same neuron shown in Ad, where arrowheads mark time points. Bb and d, statistical analysis of eIPSC peak amplitudes. Be, Stry and GBZ sensitivity of the peak amplitudes. Ca, scaled and peak-aligned eIPSCs, revealing no drug-induced change in decay kinetics. Same traces as in Ba and c. Cb, statistical analysis of τ_{decay} .

the amplitude obtained under strychnine, the reduction accounted for $40 \pm 11\%$ at P4 and $31 \pm 5\%$ at P11 (data not shown). As $\sim 30\%$ of glycine-induced currents were also blocked by $10 \mu\text{M}$ GBZ in puff application experiments (Fig. 2B), we conclude that the reduction of synaptic currents by GBZ was due to non-specific inhibition of GlyRs that had remained unblocked by 100 nM strychnine. Indeed, increasing the strychnine concentration to $1 \mu\text{M}$ completely blocked the residual currents (those remaining after wash-in of 100 nM strychnine and $10 \mu\text{M}$ GBZ; $n = 4$, data not shown). As kinetic properties of glycine-mediated currents are faster than GABA-mediated currents (Jonas *et al.* 1998; O'Brien & Berger, 1999; Russier *et al.* 2002; Awatramani *et al.* 2005; Ishibashi *et al.* 2013), one would expect a slow-down of the decay at mixed synapses after wash-in of strychnine. However, in line with our results pointing towards virtually purely glycinergic synapses, we observed no change in τ_{decay} upon strychnine or GBZ application, neither at P4 nor at P11 (Fig. 1C). Taken together, the results demonstrate a negligible GABAergic contribution to synaptic transmission and are thus in clear contrast to the earlier reports of mixed MNTB–LSO synapses in gerbils and rats (Kotak *et al.* 1998; Nabekura *et al.* 2004). However, they are in line with data obtained in juvenile mice (Giugovaz-Tropper *et al.* 2011). We conclude that exclusively glycine mediates phasic inhibitory synaptic transmission at mouse MNTB–LSO synapses, both at P4 and at P11.

Pressure-release of transmitter molecules via puff electrodes allows distinct neurotransmitter application, contrary to the scenario with coreleased GABA and glycine. We took advantage of this possibility and assessed the specificity of the blockers strychnine and GBZ. To do so, we puff-applied GABA or glycine ($100 \mu\text{M}$ each) and analysed the specificity of the blockers strychnine and GBZ (Fig. 2A). Strychnine at 100 nM did not significantly affect

GABA-evoked currents (Fig. 2B; P4: $n = 5$, $P = 0.614$; P11: $n = 5$, $P = 0.359$; paired *t* tests). By contrast, $10 \mu\text{M}$ GBZ reduced glycine-induced currents (Fig. 2B; P4: $26 \pm 5\%$, $n = 5$, $P = 0.006$; P11: $27 \pm 8\%$, $n = 5$, $P = 0.030$; paired *t* tests). We interpret this as a non-specific action of GBZ at GlyRs, consistent with previous results of GBZ-mediated GlyR blockade with an IC_{50} of $\sim 50 \mu\text{M}$ (Wang & Slaughter, 2005; Beato *et al.* 2007; Li & Slaughter, 2007). Consequently, results obtained with GBZ, similar to bicuculline-based results, need to be interpreted with some caution.

Although we found no evidence for a GABAergic component at mouse MNTB–LSO synapses, it is possible that LSO principal cells receive GABAergic input from sources other than the MNTB. In order to address a potential synaptic contribution of GABA stemming from other sources, we recorded mIPSCs from LSO principal neurons at P4 and P11. At P4, we observed mIPSCs at a rate of $1.2 \pm 0.5 \text{ s}^{-1}$ with peak amplitudes of $48 \pm 9 \text{ pA}$ and a τ_{decay} of $6.1 \pm 1.1 \text{ ms}$ (Fig. 3A and B). GBZ ($10 \mu\text{M}$) affected neither the mIPSC rate (Fig. 3Aa and b; $n = 10$; $P = 0.55$, paired *t* test), nor the peak amplitude (Fig. 3Ba and b; $n = 10$; $P = 0.20$, paired *t* test), nor τ_{decay} (Fig. 3Ba and c; $n = 10$; $P = 0.19$, paired *t* test). In contrast, bath application of strychnine ($1 \mu\text{M}$) completely abolished mIPSCs. We obtained similar results at P11. Under control conditions, the mIPSC rate amounted to $2.5 \pm 0.8 \text{ s}^{-1}$, with a peak amplitude of $84 \pm 22 \text{ pA}$ and a τ_{decay} of $4.0 \pm 0.6 \text{ ms}$ (Fig. 3C and D). In the presence of GBZ ($10 \mu\text{M}$), we observed an unchanged mIPSC rate (Fig. 3Ca and b; $n = 6$; $P = 0.272$, paired *t* test), an unchanged peak amplitude (Fig. 3Da and b; $n = 6$; $P = 0.625$, paired *t* test), and an unchanged τ_{decay} (Fig. 3Da and c; $n = 6$; $P = 0.325$, paired *t* test). mIPSCs were completely abolished in $1 \mu\text{M}$ strychnine. These results suggest an absence of functional synaptic GABA_ARs at principal LSO neurons.

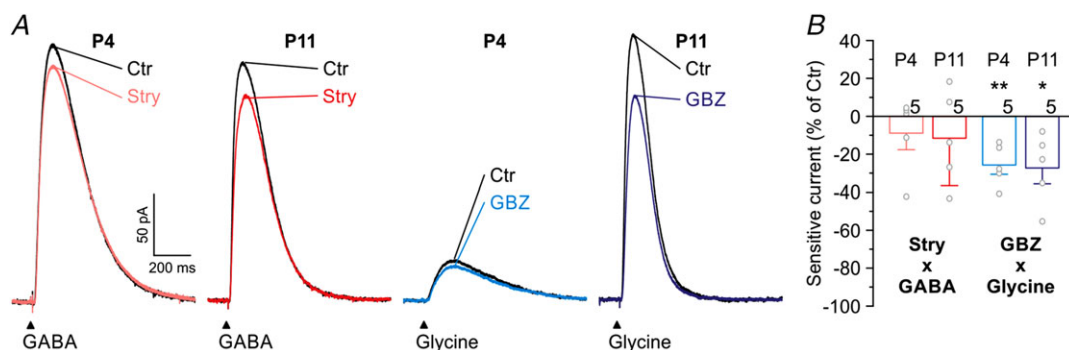


Figure 2. GlyR-mediated currents are diminished by GBZ

A, averaged current traces of four P4 and P11 LSO neurons (40 traces per neuron), evoked by application of GABA or glycine ($100 \mu\text{M}$; 100 ms puffs for 2 min at 0.2 Hz) in the absence or presence of receptor blockers. Black traces represent control conditions, and coloured traces represent recordings after 15 min wash-in of 100 nM Stry or $10 \mu\text{M}$ GBZ. B, Stry-sensitive and GBZ-sensitive fraction of GABA- and glycine-evoked currents, respectively. Strychnine at 100 nM had no effect on GABA-evoked currents. In contrast, $10 \mu\text{M}$ GBZ reduced glycine-evoked currents both at P4 and at P11 (20 cells, 5 at each age, 5 for each drug). Asterisks indicate differences from control.

In order to assess further whether functional synaptic GABA_ARs are absent at LSO principal neurons, we recorded mIPSCs in the presence of the GABA_AR modulator pentobarbital (30 μ M bath-applied). One can thus avoid the side effects of GBZ, namely cross reactivity at the counterpart receptor molecule GlyR. To

determine the decay time, we fitted a double exponential function to individual mIPSC traces, thereby revealing τ_{fast} and τ_{slow} and the respective amplitudes. From these values, we calculated the weighted τ_w (see Methods). We found no difference in τ_w between Ctr and drug, neither at P4 nor at P11 (Fig. 3E and Fa and b; P4: Ctr:

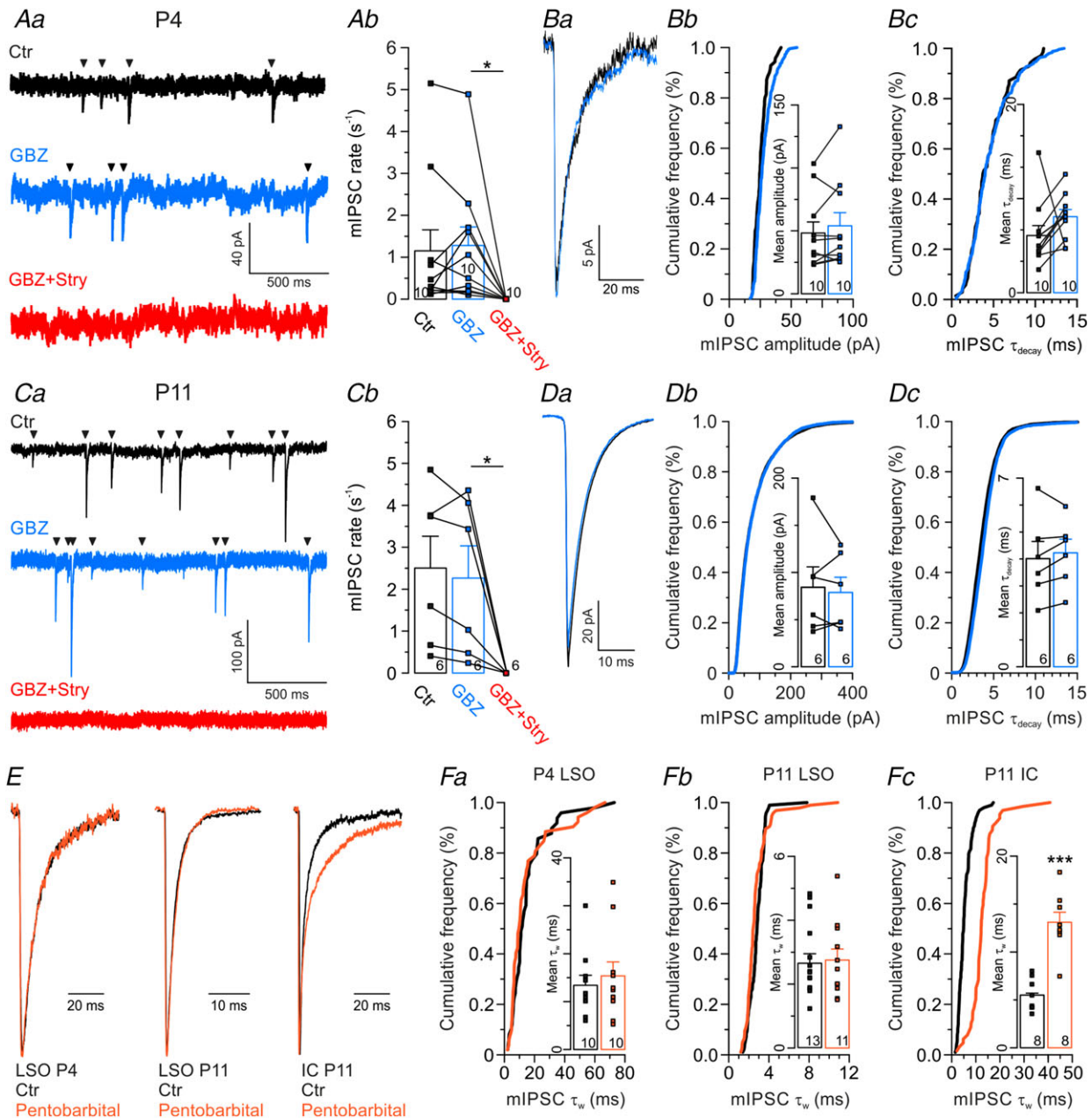


Figure 3. All inhibitory synaptic inputs to LSO neurons are mediated by glycine, not by GABA

Aa, miniature IPSCs (mIPSCs, arrowheads) from a representative P4 LSO neuron under control conditions (Ctr, black), followed by consecutive wash-in of GBZ (10 μ M, blue) and Stry (1 μ M, red). **Ab**, statistical analysis of mIPSC rate. **Ba**, averaged peak-aligned mIPSC recordings of a representative P4 LSO neuron under control conditions and in GBZ. **Bb** and **c**, statistical analysis of amplitude and τ_{decay} . Cumulative plots show a representative cell, bar diagrams show the sample. **C** and **D** same as in **A** and **B**, but for P11. **E**, average peak-scaled mIPSCs ($n = 41-147$) under control conditions (black) and in the presence of pentobarbital (30 μ M, orange) from P4 LSO (left), P11 LSO (middle) and P11 inferior colliculus (IC, right). **Fa-c**, statistical analysis of τ_w .

13.4 ± 2.1 ms, pentobarbital: 15.4 ± 2.9 ms, $P = 0.61$; P11: Ctr: 2.6 ± 0.3 ms, pentobarbital: 2.8 ± 0.3 ms, $P = 0.81$; unpaired t tests). The results further corroborate our conclusion that GlyRs, but not GABA_ARs, mediate synaptic inhibition of LSO principal cells. To check for the functional integrity of the drug, we performed additional experiments in the inferior colliculus, where pentobarbital effects have been described (Moore & Trussell, 2017). Pentobarbital prolonged τ_w of mIPSCs >2-fold (Fig. 3E and F; 5.5 ± 0.2 ms vs. 13.1 ± 1.0 ms, $P = 3.3 \times 10^{-5}$, unpaired t test), demonstrating that the drug was indeed pharmacologically functional.

The results shown in Figs 1–3 demonstrate an absence of GABA_AR-mediated synaptic transmission in the mouse LSO. We asked ourselves whether there are GABAergic synapses at all in the LSO, which, if they exist, would be silent (Charpier *et al.* 1995; Bekkers, 2005). We addressed this possibility by switching to a histological approach, in which we combined immunohistochemistry with confocal microscopy in order to check for a codistribution of gephyrin with GAD65/67. Gephyrin is a ubiquitous postsynaptic marker protein for inhibitory synapses (Kneussel & Loeblich, 2007; Specht *et al.* 2013; Tyagarajan & Fritschy, 2014), whereas GAD65/67 (the GABA-synthesizing glutamate decarboxylases GAD65 and GAD67) are presynaptic proteins at GABAergic synapses. The analysis revealed no codistribution of the two markers (Fig. 4Aa–c and Ba). We also looked for codistribution of gephyrin with GlyT2, the glycine transporter type 2, which is a presynaptic marker for glycinergic axon terminals (Friauf *et al.* 1999; Eulenburg *et al.* 2005). In contrast to the GAD65/67–gephyrin results, GlyT2 and gephyrin immunosignals were in very close proximity of as little as 78 nm (Fig. 4Ad–f and Bb). Further quantification by Pearson's coefficient and the P_{Costes} value (a measure of reliability) confirmed the absence of GAD65/67–gephyrin codistribution (Pearson's coefficient: 0.10 ± 0.01; $n = 32$; $P_{\text{Costes}} = 0.88 \pm 0.04$), yet the presence of GlyT2–gephyrin codistribution (Pearson's coefficient: 0.48 ± 0.03; $n = 23$; $P_{\text{Costes}} = 1.00 \pm 0.00$). Hence, there is no evidence for GABAergic synapses in the mouse LSO at P11, when hearing onset occurs. In order to check whether this is also the case during early development, we performed the same series of experiments at P4. We also detected gephyrin, GlyT2 and GAD65/67 (Fig. 4D). Similar to P11, fluorescence of gephyrin and GlyT2 peaked in close proximity (Fig. 4Ea). In contrast, there was no match between GAD65/67 and gephyrin fluorescence (Fig. 4Eb). Accordingly, Pearson's coefficient and P_{Costes} values showed a codistribution trend for gephyrin and GlyT2 (Fig. 4Fa and b; Pearson's coefficient: 0.32 ± 0.02; $n = 37$; $P_{\text{Costes}} = 0.90 \pm 0.04$), but no evidence towards a codistribution for gephyrin and GAD65/67 (Fig. 4Fa and b; Pearson: 0.20 ± 0.04; $n = 25$; $P_{\text{Costes}} = 0.83 \pm 0.07$).

LSO principal neurons possess functional GABA_BRs

As synaptic GABA_ARs are absent in MNTB–LSO inputs, we wondered whether other types of GABA receptors might be involved in GABA signalling and checked for pre- and postsynaptic GABA_BRs. To assess the presence of GABA_BRs, we analysed responses of LSO principal neurons to focally applied baclofen, a GABA_BR agonist (Fig. 5Aa). We observed robust outward currents with slow kinetics (Fig. 5Ab) and peak amplitudes of 35 ± 1 pA at P4 and 70 ± 5 pA at P11 (Fig. 5Ba). These baclofen-induced outward currents were virtually abolished when the GABA_BR blocker CGP was present (Fig. 5Ab), with peak amplitudes as low as 5 ± 2 pA at P4 and 10 ± 2 pA at P11 (Fig. 5Ba). The fraction of the blocked current was ~90% at both ages. Outward currents with slow kinetics are indicative of K⁺ outflux mediated by G protein-coupled inward-rectifying K⁺ channels (Lüscher & Slesinger, 2010). To assess channel contribution, we monitored R_m . During baclofen application, R_m was reduced to 74 ± 3% at P4 and to 79 ± 1% at P11 (Fig. 5C and D). R_m was unchanged when baclofen was applied in the presence of CGP (Fig. 5C and D; 104 ± 3% at P4; 101 ± 2% at P11). Together, these data suggest that LSO principal neurons possess functional GABA_BRs, at least during prehearing development and at hearing onset.

Ca²⁺ influx into MNTB axon terminals is reduced via presynaptic GABA_BRs

Next, we investigated the presence of presynaptic GABA_BRs and a possible presynaptic modulation of glycinergic MNTB–LSO synapses by these receptors, as seen in gerbils (Magnusson *et al.* 2008). Presynaptic GABA_BRs commonly suppress neurotransmitter release by inhibiting voltage-activated Ca²⁺ channels and reducing Ca²⁺ influx (Wu & Saggau, 1995; Dittman & Regehr, 1996; Takahashi *et al.* 1998; Chanda *et al.* 2011; Gassmann & Bettler, 2012). To study whether GABA_BR activation results in reduced Ca²⁺ influx into MNTB axon terminals, we performed Ca²⁺ imaging using Mg-green (Fig. 6A and B; see Methods for details). Electrical stimulation of P11 MNTB axons resulted in increased fluorescence at healthy presynaptic terminals (Fig. 6Ab and B, green ROI). No increase occurred at structures showing a fluorescent bleb or at loaded axons (Fig. 6Ab and B, blue ROI). In a similar series of experiments, we obtained recordings from the complete field of view with a photodiode, enabling us to do Ca²⁺ imaging at sub-millisecond temporal resolution from one to five loaded boutons at a time (Fig. 6C and D). A rapid increase of the Ca²⁺ signal occurred upon stimulation, followed by a fast decline with a τ_{decay} of 15.3 ± 2.4 ms (Fig. 6D; $n = 5$). Bath application of baclofen (100 μM) reversibly diminished the stimulus-evoked peak calcium response to 80 ± 3%

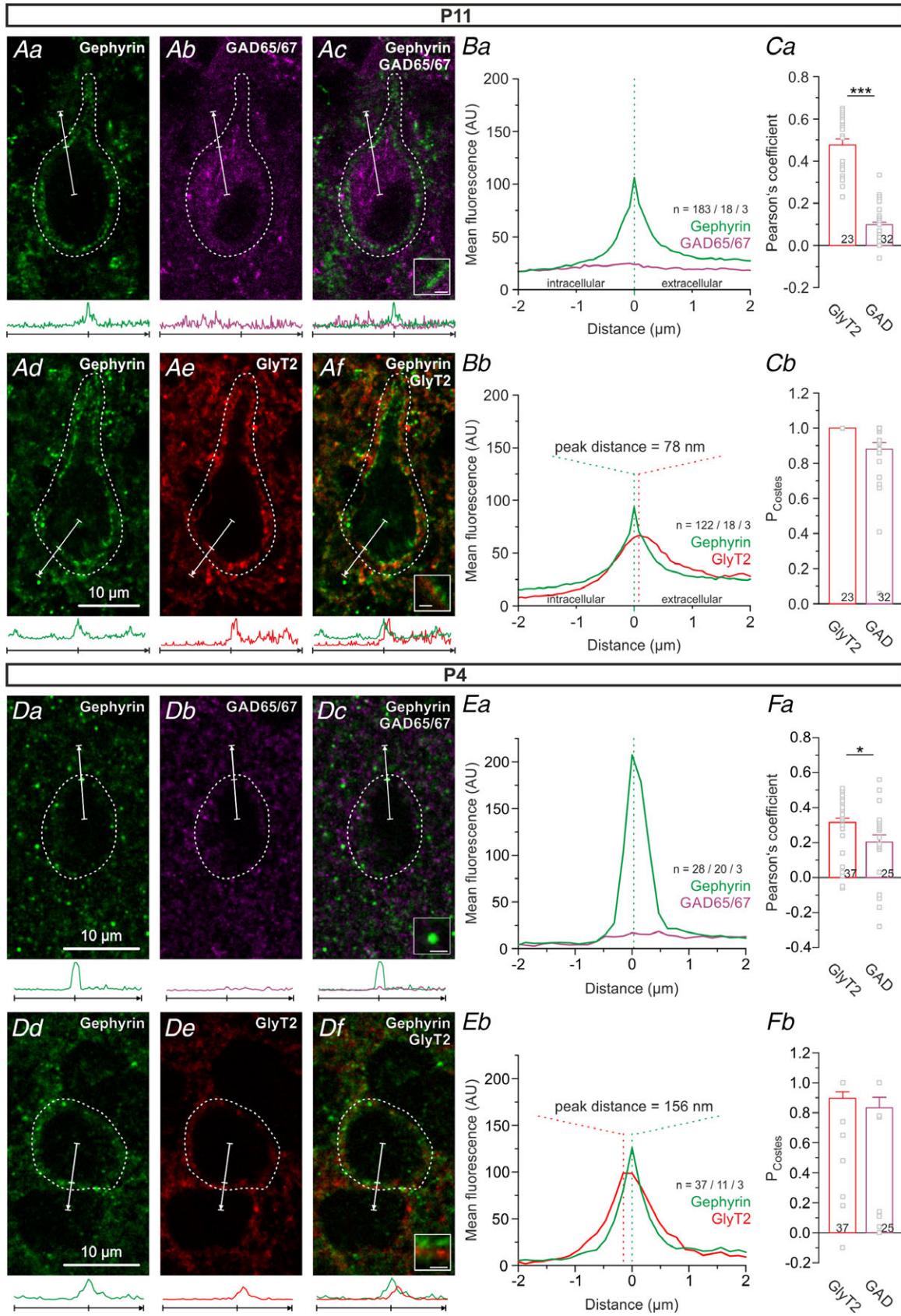


Figure 4. GlyT2, but not GAD, codistributes with gephyrin at somata of LSO principal neurons

Aa–c, immunohistochemical detection of the inhibitory postsynaptic marker gephyrin and the presynaptic GABA marker GAD65/67 at P11. Ad–f, same as a–c, but with gephyrin and the presynaptic glycinergic marker GlyT2. Merged images in panels ac and Af. Intensity profiles of the immunosignals across inhibitory synapses (bottom of Aa–f) determined by line scans originating from the soma centre and crossing membrane-associated gephyrin signals (white arrows in Aa–f, centre tick marks gephyrin signal). Ba and b, spatial distribution of gephyrin with GAD65/67 or GlyT2 as visualized by average intensity profiles. n, number of profiles/cells/animals; AU, arbitrary units. Before averaging, each profile was aligned to the position of the maximal gephyrin signal. Negative μm values demonstrate an intracellular signal, positive μm values an extracellular one; 78 nm equals the pixel width, thus indicating the closest detectable distance. Ca and b, to assess a somatic codistribution of gephyrin with GlyT2 or GAD65/67, ROIs were drawn 1–2 μm distal to the plasma membrane (dashed lines in Aa–f) and analysed for Pearson's coefficient and corresponding P_{Costes} values. Codistribution is evidenced by $P_{\text{Costes}} > 0.95$. D–F, same as A–C, but for P4. Pixel width is 156 nm instead of 78 nm.

(Fig. 6Da and b; $n = 5$, $P = 0.003$, paired t test) but did not affect τ_{decay} (Fig. 6Dc; $n = 5$, $P = 0.896$, paired t test). In conclusion, functional GABA_BRs are present on MNTB axon terminals in the LSO and their activation leads to reduced Ca²⁺ influx.

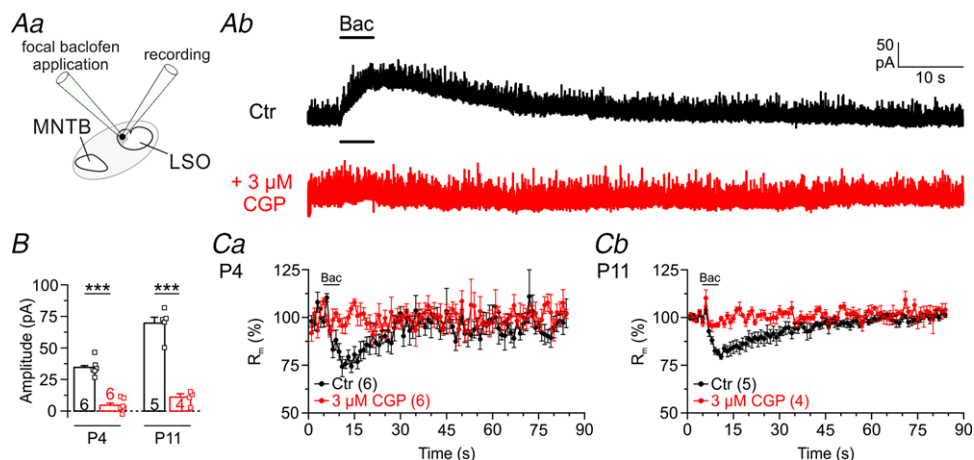
GABA_BR activation in the LSO results in reduced glycinergic eIPSCs

Reduced presynaptic Ca²⁺ influx upon GABA_BR activation reduces the release probability for synaptic vesicles, which finally results in smaller ePSC amplitudes and, likewise, weaker synaptic strength (Zucker & Regehr, 2002; Friauf *et al.* 2015). GABA_BR activation at MNTB axon terminals may thus reduce the amount of released glycine and therefore result in smaller glycinergic ePSC amplitudes in LSO neurons. We addressed this point and recorded from P4 and P11 LSO principal neurons while electrically stimulating MNTB fibres (trains of 24 pulses at 0.2 Hz). During the trains, we focally applied the GABA_BR agonist baclofen (10 μM for 5 s; Fig. 7Aa–c). Under Ctr conditions, MNTB fibre stimulation elicited robust and stable eIPSCs, most likely mediated by glycine

(Fig. 7Ab). In contrast, baclofen application resulted in substantially reduced synaptic strength (Fig. 7Ab and c). Amplitudes were reduced to $73 \pm 5\%$ at P4 and to $35 \pm 4\%$ at P11 (Fig. 7Ba and b; $n = 4, 5$). In the presence of 3 μM CGP, eIPSC amplitudes remained unchanged upon baclofen application (Fig. 7C and D). Collectively, we provide pharmacological evidence that GABA_BR activation reduces the synaptic strength (Fig. 7Da and b). Hence, we conclude that GABA modulates glycinergic synaptic transmission at mouse MNTB–LSO synapses through activating presynaptic GABA_BRs (see Giugovaz-Tropper *et al.* 2011).

GABA_AR-mediated inhibition is extrasynaptic

Although we obtained no evidence for a participation of GABA in *synaptic* transmission at mouse MNTB–LSO synapses, GABA may still be able to act at *extrasynaptic* GABA_ARs (Farrant & Nusser, 2005; Brickley & Mody, 2012). To check for the presence of functional extrasynaptic GABA_ARs in principal LSO neurons, we puff-applied GABA (100 μM) while recording whole-cell currents. Such GABA puffs consistently evoked

**Figure 5. LSO principal neurons possess functional GABA_BRs**

Aa, scheme of the experimental set-up. Ab, original traces (P11) with focal baclofen application (10 μM , 5 s) at the indicated time points in control (Ctr, black,) and CGP (3 μM , red). B, statistical analysis of peak amplitude. C and D, time course of membrane resistance.

robust responses of very similar peak amplitudes at P4 and P11 (Fig. 8Aa and b; P4: 157 ± 20 pA, $n = 11$; P11: 155 ± 18 pA, $n = 22$; $P = 0.962$, unpaired t test). When GABA was coapplied with GBZ, responses were almost completely suppressed (Fig. 8Ac; P4: $93 \pm 3\%$, $n = 5$, $P = 0.062$; P11: $99 \pm 1\%$, $n = 4$, $P = 0.391$; paired t tests compared to 100%).

GABA is a potent full agonist at GABA_ARs, yet it is merely a partial agonist at extrasynaptic receptor isoforms, particularly those containing δ subunits (δ -GABA_ARs). In contrast, THIP is a much more efficient agonist at δ -GABA_ARs (Krogsgaard-Larsen *et al.* 1994; Krogsgaard-Larsen *et al.* 2002; Orser, 2006; Olsen & Sieghart, 2008; Mortensen *et al.* 2010), displaying 'super agonist' behaviour with an E_{\max} of $\sim 160\%$ (Brown *et al.* 2002; Wohlfarth *et al.* 2002; Krogsgaard-Larsen *et al.* 2004; Drasbek & Jensen, 2006). THIP has a lower EC₅₀ value and evokes a larger maximal current at $\alpha_4\beta_3\delta$ receptors than at $\alpha_4\beta_3\gamma_2$ receptors (Brown *et al.* 2002). In order to check for functional δ -GABA_ARs, we puff-applied THIP onto somata of P11 LSO principal neurons. In contrast to others (Hoestgaard-Jensen *et al.* 2014, 100 μ M), we used a much lower concentration of 1 μ M to minimize side effects such as THIP's antagonistic activity at ρ_{1-3} subunits (Johnston *et al.* 2003; Alexander *et al.* 2017).

Despite the low concentration, much lower than the EC₅₀ of 44 μ M (Drasbek & Jensen, 2006), we observed tonic inward currents of -13 ± 2 pA (Fig. 8B; $n = 10$, $P = 1.2 \times 10^{-4}$, paired t test). Their peak amplitudes were in the expected range for δ -GABA_ARs under high internal Cl⁻ (Meera *et al.* 2011). The addition of GBZ (100 μ M) reduced the tonic inward currents to -8 ± 2 pA ($n = 10$, $P = 4.7 \times 10^{-4}$, paired t test), and washout conditions were again indistinguishable from controls ($n = 10$, $P = 0.499$, paired t test). Based on these pharmacological results, we conclude that LSO principal neurons possess functional extrasynaptic GABA_ARs.

We next assessed the relative abundance of all GABA_AR subunit transcripts in the LSO. To do so, we coupled laser capture microscopy with global transcriptome profiling. We detected 13 of the 19 different transcripts (Fig. 9). *Gabra5*, which codes for the α_5 subunit, was most abundant, followed by *Gabrd*, which codes for the δ subunit. Both subunits are components of extrasynaptic GABA_ARs (Brickley & Mody, 2012; Knoflach *et al.* 2016) and mediate tonic inhibition (Thomas *et al.* 2005; Glykys *et al.* 2008). δ -GABA_ARs are exclusively located at perisynaptic and extrasynaptic sites (Wei *et al.* 2003; Semyanov *et al.* 2004; Farrant & Nusser, 2005; Mody, 2005), where they form α_4/α_6 -containing receptors (Karim *et al.* 2012).

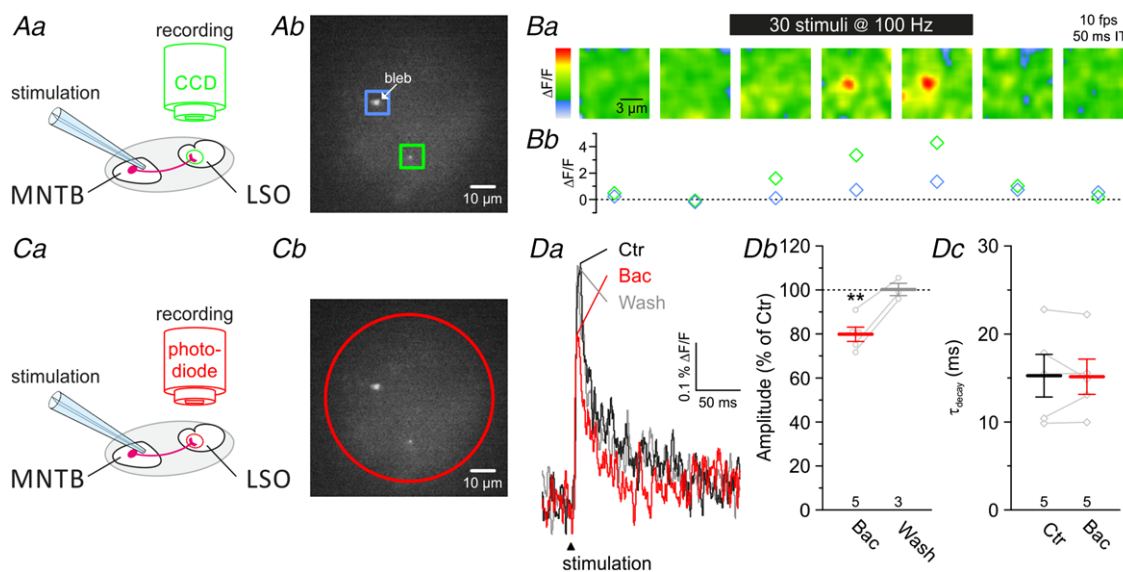


Figure 6. Presynaptic Ca^{2+} influx at MNTB–LSO synapses is controlled by GABA_BRs

A and C, loading of MNTB fibres with the Ca^{2+} indicator Mg-green resulted in labelled presynaptic axon terminals in the LSO (Ab and Cb). Ca^{2+} imaging during electrical stimulation of MNTB–LSO fibres (Aa) enables spatial recordings from labelled presynaptic terminals (Ab, green and blue ROIs) in the LSO with a temporal resolution of 10 frames s^{-1} (fps, Ba). Integration time (IT) for a single frame was 50 ms. The green ROI in Ab frames a Mg-green positive, healthy presynaptic terminal, which is also shown during stimulation in Ba. The relative change in fluorescence ($\Delta F/F$) of this terminal upon 100 Hz stimulation is depicted in Bb (green), together with a large bleb (blue, blue frame in Ab). Noise in Ba was removed with a Gaussian filter (radius 6 pixels). Photodiode recordings (Ca and red circle in Cb) allowed Ca^{2+} imaging in the sub-millisecond range. D, average Ca^{2+} responses ($n = 40$ in each case) upon MNTB–LSO fibre stimulation at 0.2 Hz (Da) under control conditions (Ctr, black) became reversibly diminished in amplitude (Db) in the presence of 100 μ M baclofen (+Bac, red). Wash-out (wash) of 15 min of Bac is depicted in grey. Kinetics of Ca^{2+} influx was unaffected in the presence of Bac (Dc).

α_5 subunits are typically associated with γ_2 and β_1 subunits (Walker & Semyanov, 2008), and *Gabrg2* and *Gabrb1* transcripts coding for the latter subunits were among the most abundant counts. Together, our profiling results provide further evidence for the existence of extrasynaptic GABA_ARs in the LSO.

Extrasynaptic GABAergic inhibition depends on GAT-1/3 activity

GATs are responsible for GABA reuptake, but these transporters can also work in the reverse direction, thereby elevating extracellular GABA levels (Richerson & Wu,

2003; Heja *et al.* 2009; Unichenko *et al.* 2013). As functional GAT-1 and GAT-3 are present in the LSO (Stephan & Friauf, 2014), we hypothesized that GAT-1/3 activity may affect extrasynaptic GABAergic currents at LSO neurons. If GATs take up GABA, GAT blockade should foster extracellular GABA buildup, causing GABA_AR desensitization and prolonged activation of GABA_AR (Jones & Westbrook, 1995; Brickley *et al.* 1999; Mortensen *et al.* 2010). When we puff-applied GABA (100 μ M; 24 pulses at 0.2 Hz), we observed robust inhibitory currents of 820 ± 71 pA that did not change between pulse no. 1 and no. 24 (Fig. 10Aa and b and Bc; $n = 34$, $P = 0.104$, paired t test). The τ_{decay} was 267 ± 12 ms (Fig. 10Cb) and

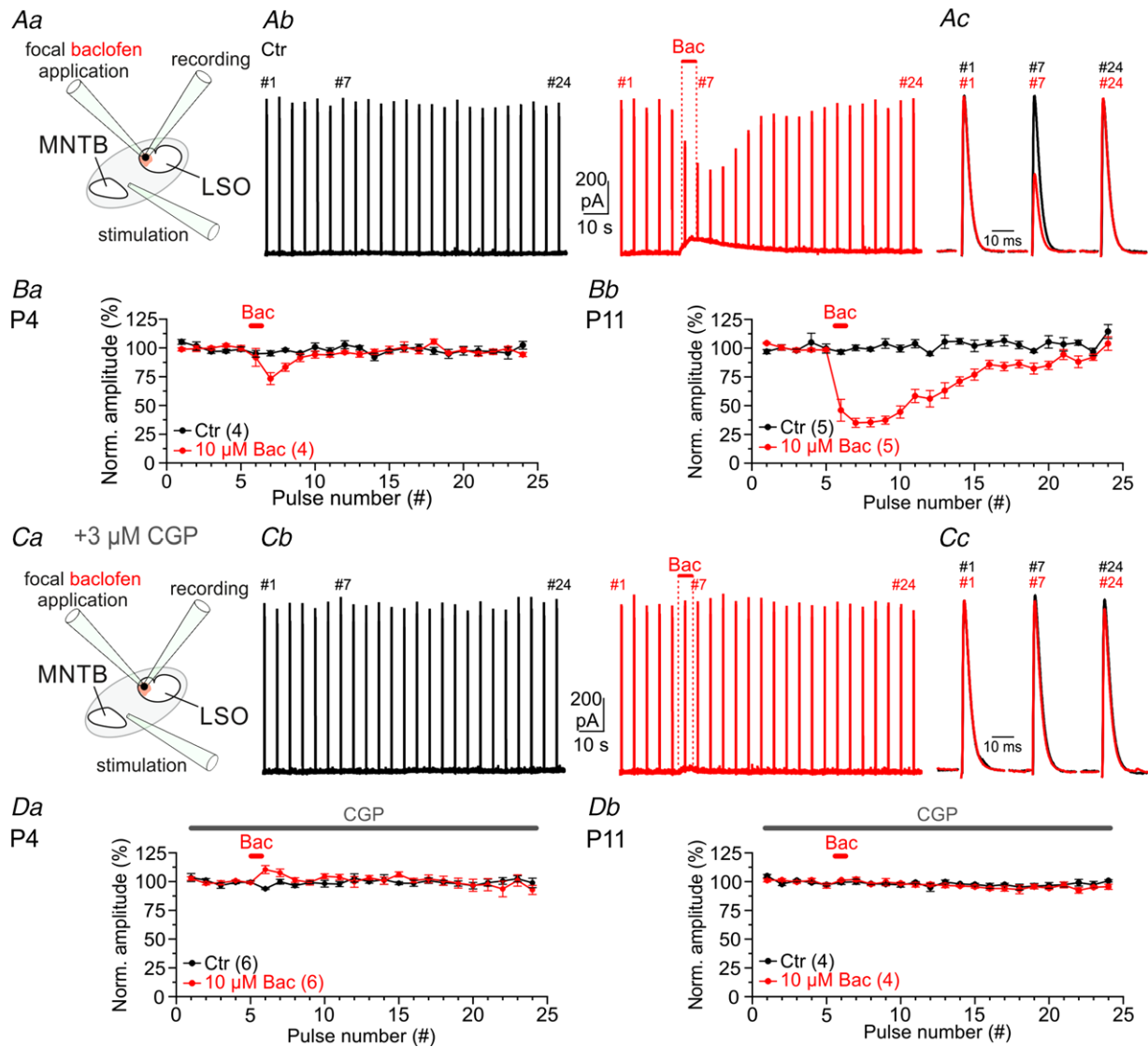


Figure 7. Activation of GABA_BRs decreases eIPSC amplitudes at MNTB-LSO synapses

Aa, scheme of the experimental set-up. Ab, MNTB fibre stimulation at P11 (24 pulses, 0.2 Hz) in control (Ctr, black) and focal baclofen application (10 μ M Bac, 5 s, red). Traces are averages of three repeats. Ac, close ups of eIPSCs at the pulse no. 1, 7 and 24 also denoted in Ab. B, quantification of normalized eIPSC amplitudes (mean of first five pulses set to 100%) at P4 (Ba) and P11 (Bb). Bc and D, same as A and B, but in the presence of bath-applied 3 μ M CGP.

remained constant during the 2 min stimulus period (Fig. 10A*b*; $n = 34$, $P = 0.088$, paired t test). Inhibition of GAT-1 with 10 μM NO-711 affected neither the amplitude (Fig. 10B*b* and *c*; $n = 8$, $P = 0.691$, paired t test) nor τ_{decay} of pulse no. 1 (Fig. 10C*a* and *b*; $n = 8$, $P = 0.711$, unpaired t test). By contrast, inhibition of GAT-3 with 40 μM SNAP-5114 reduced amplitudes by $17 \pm 4\%$ from pulse no. 1 to no. 24 (Fig. 10B*a-c*; $n = 13$, $P = 7.9 \times 10^{-4}$, paired t test) and caused a 1.9-fold slower decay (Fig. 10C*a* and *b*; $\tau_{\text{decay}} = 500 \pm 29$ ms, $n = 13$, $P = 2.9 \times 10^{-11}$, unpaired t test). A possible mechanism for this reduction is increased GABA_AR desensitization by prolonged elevated GABA levels, which are strongly regulated by GAT-3 (Dalby, 2000). Coapplication of NO-711 with SNAP-5114 caused yet stronger reduction of GABA currents by $55 \pm 4\%$ (Fig. 10B*a-c*; $n = 9$, $P = 1.4 \times 10^{-6}$, paired t test) from pulse no. 1 to no. 24 and a concomitant increase of τ_{decay} of pulse no. 1 to 757 ± 61 ms (Fig. 10C*a* and *b*; $n = 8$, $P = 6.4 \times 10^{-5}$, unpaired t test). The more than additive effect points to a synergistic action of GAT-1 and GAT-3 in regulating GABA. To test whether the reduction was a result of GABA_AR desensitization, rather than a

different GABA target, we tested the effects of 100 μM muscimol, a GABA_AR agonist not transported by GAT-1 and GAT-3 (Keros & Hablitz, 2005; Madsen *et al.* 2010). Puff application of muscimol mimicked the situation of NO-711 and SNAP-5114 coapplication. Amplitudes were depressed by $75 \pm 5\%$ from pulse no. 1 to no. 24 (Fig. 10B*a-c*; $n = 9$, $P = 3.3 \times 10^{-8}$, paired t test) and τ_{decay} of pulse no. 1 increased to 1.11 ± 0.15 s (Fig. 10C*a* and *b*; $n = 9$, $P = 5.8 \times 10^{-4}$, unpaired t test). These results suggest that receptor desensitization, resulting from prolonged agonist exposure, specifically causes the reduction. Collectively, they demonstrate a functional role of astrocytic GATs in regulating extracellular GABA levels in the mouse LSO.

Extrasynaptic GABA decreases the excitability of LSO neurons with low $[\text{Cl}^-]_i$

In contrast to subsynaptic GABA_ARs, extrasynaptic GABA_ARs respond to low concentrations of ambient GABA, thus generating a tonic conductance (Farrant & Nusser, 2005; Brickley & Mody, 2012). To complement

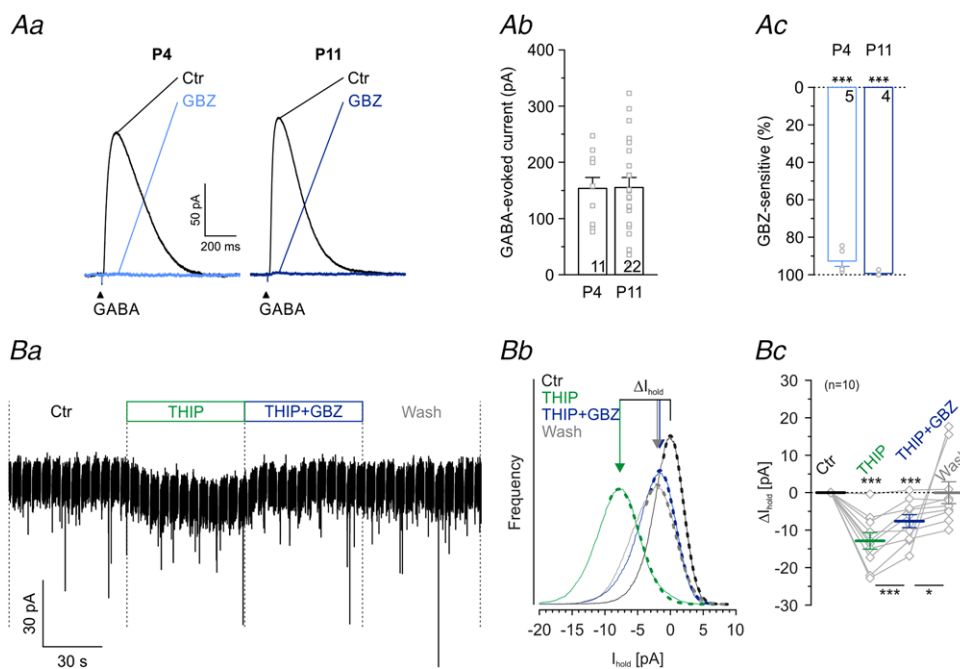


Figure 8. LSO principal neurons possess extrasynaptic δ -GABA_ARs

A*a*, averaged current traces ($n = 40$) of a P4 and a P11 LSO neuron, evoked by GABA application (100 μM ; 100 ms puffs for 2 min at 0.2 Hz). Black traces represent control conditions, and grey traces represent recordings after 15 min wash-in of 10 μM GBZ. A*b*, amplitude distribution of GABA-evoked currents at P4 and P11. A*c*, Sensitivity to GBZ at P4 and P11. B*a*, current traces during puff application of the δ -GABA_AR agonist THIP (1 μM), demonstrating a long-lasting inward current that was partially blocked with GBZ. Significance levels were Šidák corrected in case of two comparisons. B*b*, same cell as in B*a*. The holding current (I_{hold}) was determined from Gaussian fits (dashed lines) to all-point histograms (solid lines) of the different pharmacological conditions. Due to the high internal chloride concentration, both inhibitory and excitatory spontaneous synaptic current events are inward directed. To exclude those inward-directed events, Gaussian fitting was done at the right side of the all-point histograms. B*c*, statistics of THIP-evoked currents and sensitivity to GBZ ($n = 10$ cells). Asterisks above dashed line depict differences from control. Significance levels were Šidák corrected in case of two comparisons.

our view of the action of inhibitory transmitters in the LSO, we finally addressed the impact of tonic GABAergic inhibition on the excitability of LSO neurons. To do so, we injected 10 s current pulses, stepwise increasing the current amplitude until an action potential was elicited. We did this in control conditions and during GABA puffs at various concentrations (Fig. 11Aa and b). GABA at 1 μM was insufficient to cause changes in the resting membrane potential (V_M) or in I_{AP} , the current amplitude required to elicit an action potential (Fig. 11Ac and d; $P = 0.451$ and $P = 0.102$, $n = 8$, paired t test). In the presence of 10 μM GABA, however, the firing threshold was reached at a higher current amplitude than in controls (Fig. 11Aa and d). Notably, 1 μM and 10 μM GABA are in the physiological range (Attwell *et al.* 1993; Morishima *et al.* 2010). We observed a tonic hyperpolarization (ΔV_M) of -1.9 ± 0.4 mV ($n = 6$, $P = 0.005$, paired t test) and a concurrent shift of I_{AP} (ΔI_{AP}) amounting to 67 ± 17 pA ($n = 6$, $P = 0.010$, paired t test). The effects were stronger at 100 μM GABA (Fig. 11Ac and d; ΔI_{AP} : 625 ± 108 pA; ΔV_M : -3.3 ± 0.5 mV; $P = 0.002$ and $P = 0.002$, $n = 6$, paired t test). All effects were abolished when GABA was coapplied with GBZ (Fig. 11Ac and d). Compared to 10 μM GABA, 100 μM GABA led to a 1.7-fold increased ΔV_M , yet to a 9.3-fold increased ΔI_{AP} . As the disproportionately high increase of ΔI_{AP} may be due to a reduced membrane resistance (R_M), we calculated R_M during control condition and during GABA application (Fig. 11Ba and b). Under control conditions, R_M averaged

55 ± 8 M Ω ($n = 19$), but it dropped by $21 \pm 3\%$ during application of 10 μM GABA (Fig. 11Bb and c; $n = 6$, $P = 5.1 \times 10^{-4}$, paired t test). When GABA was raised to 100 μM , R_M dropped by $54 \pm 5\%$ ($n = 5$, $P = 3.4 \times 10^{-4}$, paired t test). The effect was abolished upon coapplication of GABA with GBZ. Collectively, these results show that the GABA-induced decrease of R_M is in line with a decreased excitability of LSO neurons mediated through GABA_ARs.

Extrasynaptic GABA increases the excitability of LSO neurons with high [Cl⁻]_i

GABA and glycine can be depolarizing and even excitatory in immature neurons (Kasyanov *et al.* 2004). The effect is also observed in the LSO and can be attributed to a high [Cl⁻]_i and a reversal potential (E_{Cl}) more positive than V_M (Ehrlich *et al.* 1999; Balakrishnan *et al.* 2003; Löhrlke *et al.* 2005). We therefore wondered whether tonic, extrasynaptic GABA effects might increase the excitability at early developmental stages. We addressed the question by performing experiments at P4 similar to the P11 experiments illustrated in Fig. 11. To mimic the native intracellular Cl⁻ concentration (Ehrlich *et al.* 1999), patch pipettes contained 32 mM Cl⁻ (consequently, $E_{Cl} = -35$ mV). As expected for such conditions, GABA puffs (10 μM) depolarized V_M by 6.8 ± 1.0 mV (Fig. 12A and B; $n = 10$, $P = 0.0001$, paired t test). Moreover, the excitability of LSO neurons increased during GABA

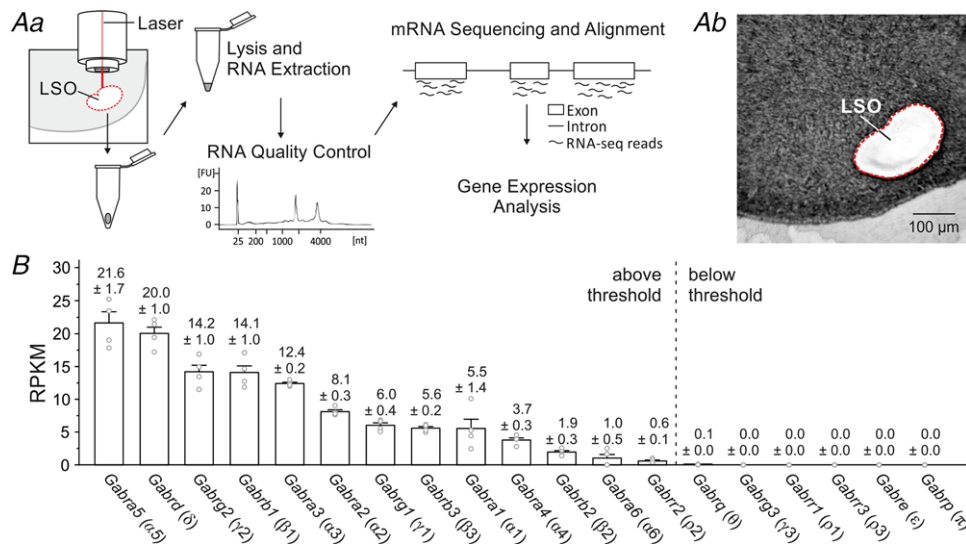


Figure 9. Transcripts *Gabra5* and *Gabrd*, coding for the extrasynaptic GABA_AR subunits $\alpha 5$ and δ , are most abundant in the mouse LSO

Aa, LSO tissue was collected via laser capture microdissection. After lysis and total RNA extraction, RNA quality control, mRNA sequencing, alignment and gene expression analysis were performed. FU, fluorescence units; nt, nucleotides. Bb, coronal brainstem slice after microdissection of the LSO. B, RPKM values (reads per kilobase per million) of 19 transcripts coding for GABA_AR subunits in the LSO ($n = 4$ for each transcript). Numbers above columns depict mean RPKM values \pm SEM; corresponding protein subunits are depicted in brackets. Genes positioned left of the dashed line were expressed above threshold.

application, as evidenced by lower current amplitudes required to elicit an action potential (Fig. 12A and C; $\Delta I_{AP} = -55.0 \pm 19.3$ pA, $n = 10$, $P = 0.020$, paired t test). The increased excitability was observed although R_M dropped by $63.5 \pm 4.5\%$ (Fig. 12D; $n = 10$, $P = 3.1 \times 10^{-7}$, paired t test), arguing against shunting inhibition as a major effect of ambient GABA at immature LSO neurons.

Discussion

Five major results have emerged from the present study (Fig. 13). First, fast inhibitory synaptic transmission in the mouse LSO appears to be mediated exclusively by glycine. Second, synaptic GABA_ARs appear to be missing in the MNTB–LSO circuit. Third, GABA modulates presynaptic

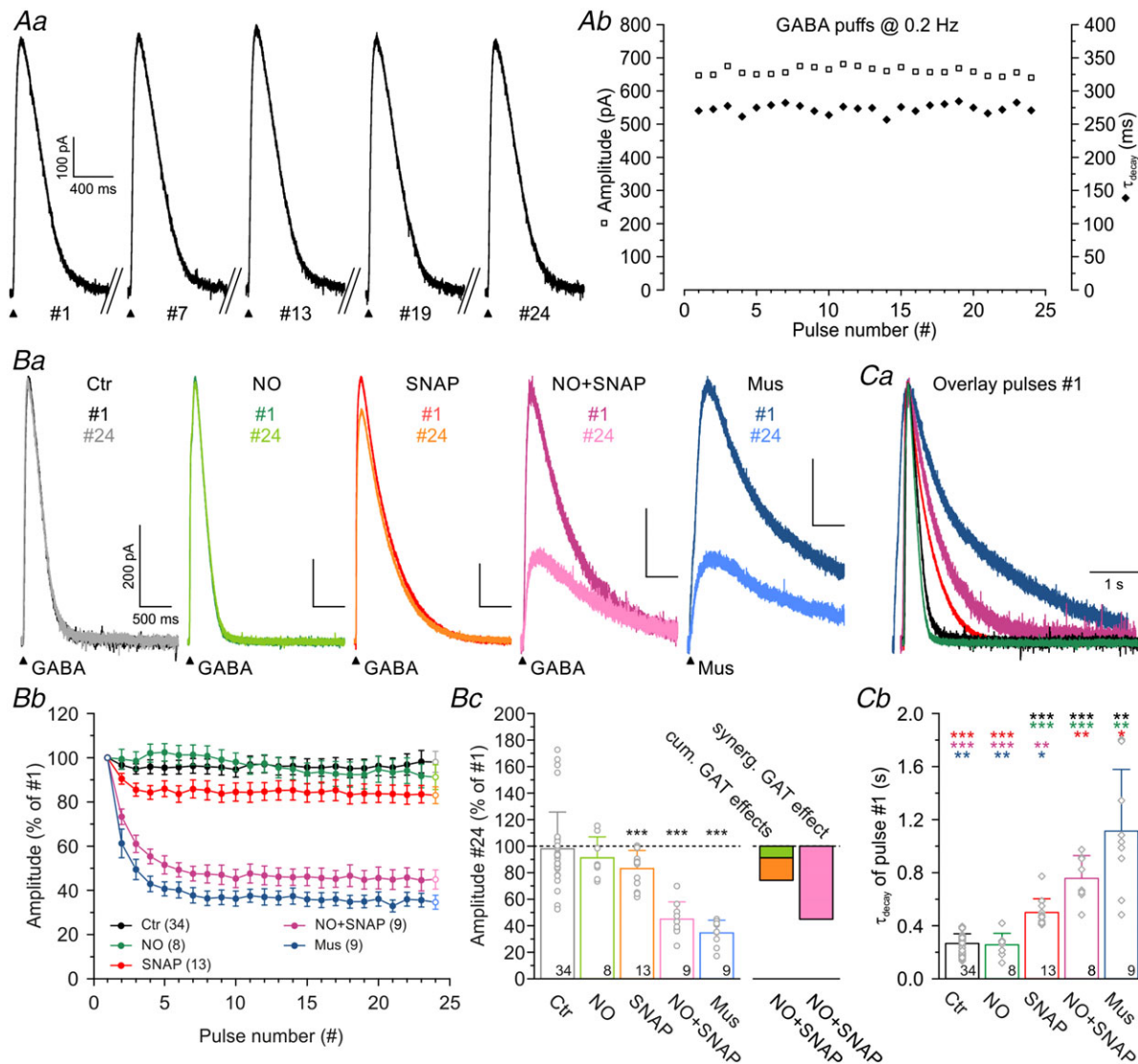


Figure 10. Extracellular GABA is synergistically controlled by GABA transporters GAT-1 and GAT-3

Aa, current traces of a P11 LSO neuron, evoked by GABA application ($100 \mu\text{M}$, 100 ms puffs for 2 min at 0.2 Hz). The pulse number (#) is provided under each trace. Ab, peak amplitudes and τ_{decay} of the evoked events as a function of time, demonstrating low amplitude jitter (squares) and stable decay kinetics (diamonds). Ba, events from pulse no. 1 to pulse no. 24 under various pharmacological conditions. Drugs were bath-applied 10 min before puff applications and were also contained in the puff pipettes. Bb, peak amplitudes did not change in the control condition. Blockade of GAT-1 ($10 \mu\text{M}$ NO-711) caused no amplitude reduction and blockade of GAT-3 ($40 \mu\text{M}$ SNAP-5114) caused a weak one. Coapplication of the two blockers, however, revealed a synergistic effect. Substitution of muscimol (Mus, $100 \mu\text{M}$) for GABA mimicked the effect of coapplied NO-711 and SNAP-5114. Bc, statistics for the data shown in Bb. Ca, scaled and peak-aligned IPSCs under various pharmacological conditions, illustrating the differences in decay kinetics. Same colour code as in Ba. Cb, statistical analysis of τ_{decay} of pulse no. 1. Colours of asterisks mark the dataset to which the comparison was made. Significance levels were Šidák corrected in case of four comparisons.

Ca²⁺ influx through presynaptic GABA_BRs, which results in weaker synaptic strength. Fourth, postsynaptic GABA_BRs mediate slow outward currents and GAT-1 and GAT-3 synergistically control extracellular GABA levels. Fifth, ambient GABA reduces the excitability of P11 LSO neurons, presumably via extrasynaptic α_5/δ -GABA_ARs, resulting in spike suppression. By contrast, ambient GABA increases the excitability at P4, resulting in spike facilitation. Notably, the increased excitability occurs when the immature network undergoes synaptic refinement and Cl⁻-mediated neurotransmission is still depolarizing.

Fast synaptic inhibition in the mouse LSO is purely glycinergic

We found glycine-mediated synaptic inhibition of LSO neurons at P4 as well as P11, in agreement with others (Kandler & Friauf, 1995; Kotak *et al.* 1998; Nabekura *et al.* 2004; Kim & Kandler, 2010). However, our results that glycine alone, without the contribution of GABA, mediates fast inhibitory synaptic transmission at mouse MNTB–LSO synapses are in contrast to findings in rats and gerbils. There, predominant GABA release has been

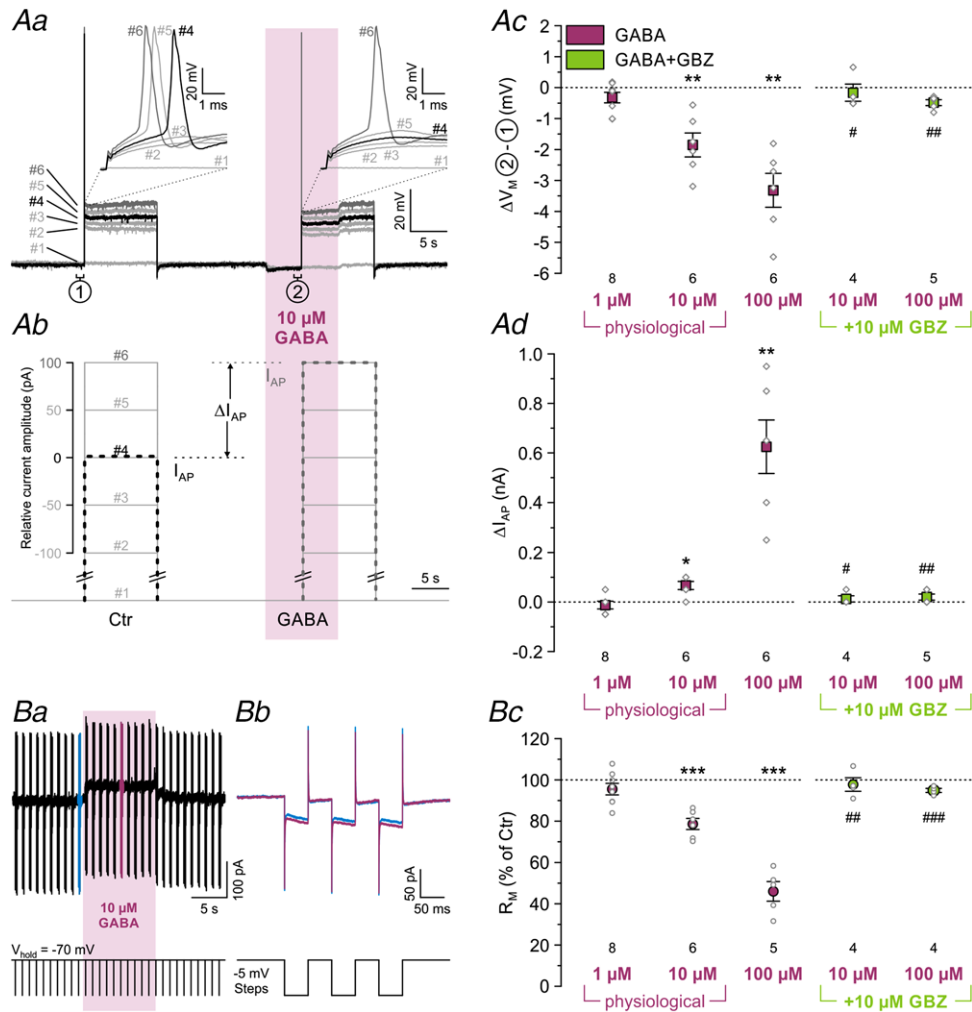


Figure 11. Tonic GABA reduces the excitability of P11 LSO neurons through extrasynaptic GABA_ARs
 Aa and b, voltage responses of a representative P11 LSO neuron to rectangular current injections with increasing amplitude (10 s duration, 6 steps). In controls, an action potential could first be elicited at pulse no. 4 (black trace), whereas a higher current amplitude was required in the presence of GABA (10 s puff; purple zone), namely at pulse no. 6 (dark grey trace). I_{AP} depicts the increase in current amplitude required to elicit an action potential; (1) and (2) mark the 1 s intervals during which the resting membrane potential (V_M) was determined. Notably, GABA also hyperpolarized the neuron. Ac, statistical analysis of ΔV_M at three GABA concentrations and during coapplication of GABA+GBZ (green). Ad, statistical analysis of I_{AP} . Ba, exemplifying 30 s current trace (top), demonstrating the effect of tonic GABA (10 μ M, 10 s puff, purple zone). To assess R_M , hyperpolarizing voltage steps of 5 mV were applied at 1 Hz (bottom) in triplets (enlargements in Bb, details in Methods) in the absence and presence of GABA (blue and purple, offset-corrected in Bb). Bc, statistical analysis of R_M . Asterisks indicate significance levels between GABA and control; hashtags indicate significance levels between GBZ+GABA and GABA.

reported in neonates, and a developmental shift (Kotak *et al.* 1998) or switch (Nabekura *et al.* 2004) from GABA to glycine has been postulated. We obtained no evidence for such a shift at mouse MNTB–LSO synapses, and our immunohistochemical data, which demonstrate no GAD65/67 codistribution with gephyrin, regardless of age, corroborate the physiological results, as they point towards a lack of GABAergic synapses in the LSO.

Pharmacological considerations

So-called GABA_AR and GlyR antagonists (GBZ, bicuculline; strychnine) also act non-specifically at the counterpart receptor molecules. Therefore, separation of GABAergic and glycinergic contributions at mixed synapses is a challenging task. Due to non-specific inhibition of GlyRs by 10 μ M bicuculline (Jonas *et al.* 1998; Nabekura *et al.* 2004), we reason that Nabekura and colleagues may have overestimated the GABA-mediated component at rat MNTB–LSO synapses. Evaluating their findings (cf. their Fig. 1c) leads us to conclude that these synapses appear to lose most, if not all, of their GABAergic characteristics before P7. In gerbils, only the medial, high-frequency limb of the LSO showed a GABA-mediated component (Kotak *et al.* 1998). Again, the authors possibly overestimated this component due to the non-specific action of bicuculline. Results from the pharmacological experiments by Kotak and collaborators, in which 2 μ M strychnine was applied initially, are more conclusive. At this concentration, strychnine most likely blocked all GlyRs and some of the GABA_ARs. The remaining current was subsequently abolished completely by 10 μ M bicuculline, providing compelling evidence for the existence of a GABAergic component in the medial limb of the gerbil LSO until P8–11. In the present study, we applied strychnine not only at 100 nM, but also 10-fold higher. As GABA_ARs are only partially blocked by 1 μ M strychnine (Jonas *et al.* 1998), a residual GABA-mediated

component would have remained if GABA_ARs were present. This, however, was not the case. Instead, we observed a complete blockade of eIPSCs upon 1 μ M strychnine (not shown). Interestingly, in contrast to Kotak and colleagues, others (Walcher *et al.* 2011) found almost no effect on MNTB–LSO transmission in P10 gerbils with 10 μ M GBZ, indicating only a minor contribution of GABA_ARs at this age, if at all. The virtual absence of GABA-mediated currents in the lateral, low-frequency limb of the gerbil LSO (Kotak *et al.* 1998) is consistent with our results. Nevertheless, we observed no GABA-mediated synaptic currents along the tonotopic axis of the LSO (data not shown). Taken together, there are some discrepancies in the literature, which we cannot completely resolve at present.

Typically, GABAergic currents decay more slowly than those mediated by glycine (Russier *et al.* 2002; but see Moore & Trussell, 2017). Remarkably, Nabekura and colleagues (2004) reported extremely long-lasting eIPSCs in rat LSO neurons (≥ 500 ms at P7, ≥ 200 ms at P14; no information about temperature). Drastically shorter durations were demonstrated at MNTB–LSO synapses of gerbils (> 160 ms at P4, ~ 80 ms at P14; Kotak *et al.* 1998; ~ 20 ms at P8–15; Sanes, 1993; ~ 20 ms at P10; Walcher *et al.* 2011). Shorter durations were also described in mice (~ 10 ms at P10; Walcher *et al.* 2011; ~ 10 ms at P11; Kramer *et al.* 2014; ~ 20 ms at P11–15; Giugovaz-Tropper *et al.* 2011; ~ 100 ms at P4, ~ 20 ms at P11, present study, Fig. 1). The values vary widely, even within the same species, but appear to decrease with age. Thus, there is some further discrepancy concerning the nature of these IPSCs that we cannot explain. We like to emphasize that GABA-mediated and glycine-mediated IPSCs are not mutually exclusively associated with long and short decay times, respectively. Rather, long decay times of ~ 80 ms, and thus long-lasting IPSCs, are also compatible with GlyRs containing α_2 subunits (Takahashi *et al.* 1992; Ghavanini *et al.* 2006). Such α_2 -GlyRs

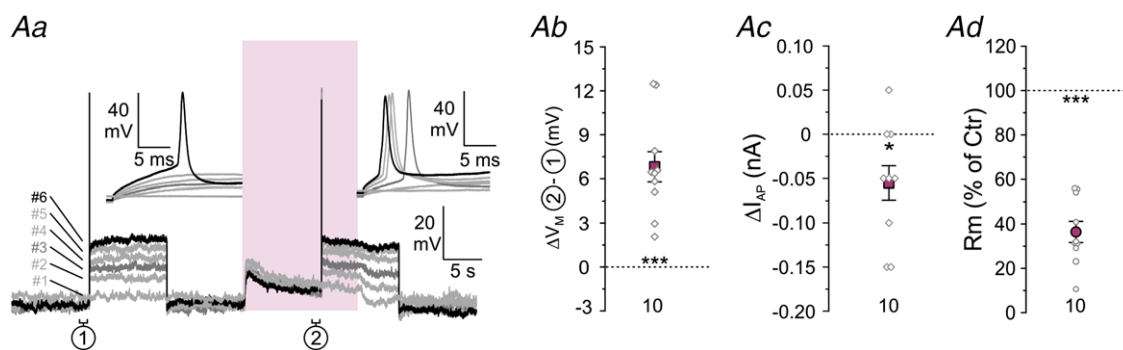


Figure 12. Tonic GABA increases the excitability of P4 LSO neurons through extrasynaptic GABA_ARs
 Aa, voltage responses of a representative P4 LSO neuron to rectangular current injections with increasing amplitude. In controls, an action potential could first be elicited at pulse no. 6 (black trace), whereas a lower current amplitude was required in the presence of 10 μ M GABA (15 s puff; purple zone), namely at pulse no. 3 (dark grey trace). Notably, GABA also depolarized the neuron. Ab–d, statistical analysis of ΔV_M (Ab), ΔI_{AP} (Ac) and R_M (Ad).

represent the ‘neonatal’ isoform and are characterized by low binding affinity for strychnine (Becker *et al.* 1988). During postnatal development of the brainstem, α_2 -GlyRs are replaced by α_1 -GlyRs (Friauf *et al.* 1997; Kungel & Friauf, 1997; Piechotta *et al.* 2001), and the replacement is accompanied by rapidly decaying synaptic responses and, consequently, speeding of glycinergic transmission (Singer *et al.* 1998; Pilati *et al.* 2016). Thus, an age-dependent acceleration of IPSCs does not necessarily

imply a decrease in the GABAergic component. It is also compatible with our observation of purely glycinergic inhibition in the developing mouse MNTB–LSO synapses. In summary, developing MNTB–LSO synapses may well display species-specific differences in the transmitter phenotype, yet we think that the GABA contribution is overestimated and less general than previously anticipated. One way to address the issue would be to perform pentobarbital experiments in gerbils and rats as we have done in the present study (Fig. 3).

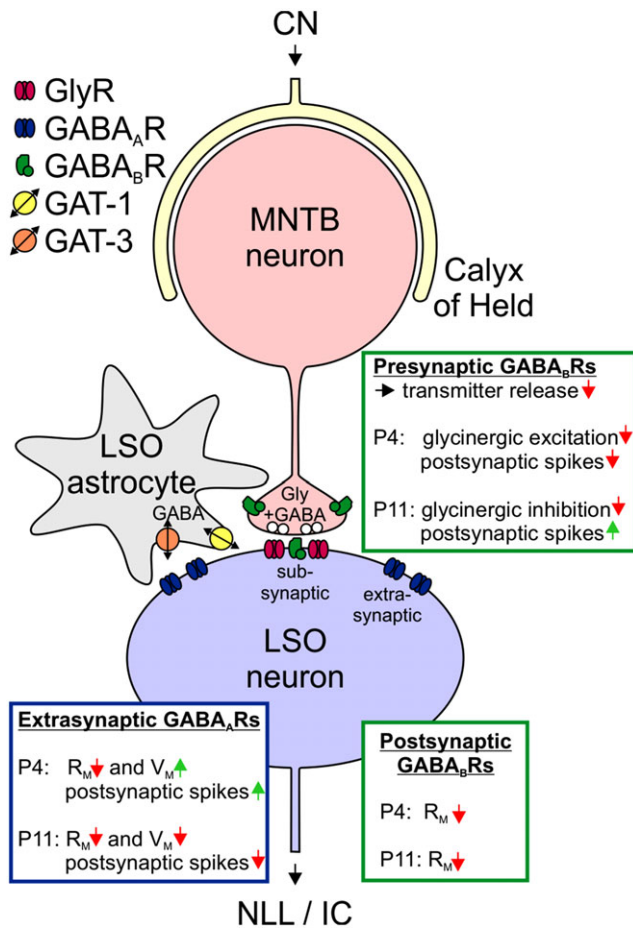


Figure 13. Schematic summary illustrating transmission at MNTB–LSO synapses of mice
MNTB neurons (red) receive excitatory input from the contralateral CN via a calyx of Held (light yellow) and convey inhibitory information to LSO principal neurons (blue) via bouton-type synapses. LSO neurons in turn innervate mesencephalic auditory nuclei like the nucleus of the lateral lemniscus (NLL) and the inferior colliculus (IC). GABA and glycine may be coreleased from MNTB–LSO synapses, but *synaptic* signalling appears to be purely glycinergic, i.e. subsynaptic receptors are GlyRs, but not GABA_ARs. MNTB axon terminals possess presynaptic GABA_BRs, LSO neurons possess extrasynaptic GABA_ARs and GABA_BRs. Extrasynaptic GABA_ARs may be activated by GABA spillover from the synaptic cleft or by reverse transport activity of astrocytic GAT-1/3. Age-specific effects mediated through presynaptic and postsynaptic GABA_BRs as well as extrasynaptic GABA_ARs are summarized in the green and blue boxes. R_M , membrane resistance; V_M , membrane potential.

GABA is a modulator

Instead of acting synaptically, GABA acts as a modulator at the glycinergic MNTB–LSO circuit. The modulation occurs via three pathways: (1) via extrasynaptic GABA_ARs, the excitability of LSO neurons is changed in an age-dependent manner; (2) via presynaptic GABA_BRs, the transmitter release from MNTB axons is reduced; and (3) via postsynaptic GABA_BRs, the membrane resistance of LSO neurons is changed. It appears that GABAergic modulation in the MNTB–LSO circuit is not a unique property of mice. *In vivo* activation of GABA_BRs at gerbil MNTB axon terminals shifts the ILD function by suppressing eIPSCs via a mechanism similar to the one demonstrated in the present study (Magnusson *et al.* 2008). eIPSC suppression mediated by presynaptic GABA_BRs is present in the projection from the MNTB to the medial superior olive of gerbils (Stange *et al.* 2013). These modulatory effects in gerbils, together with the overestimation of the synaptic GABA component (Nabekura and Kotak studies), imply that modulatory effects of GABA seem to be general in the auditory brainstem.

Sources of GABA in mouse LSO

What might be the main source of ambient GABA responsible for tonic activity in the mouse LSO? It is unlikely that MNTB axon terminals corelease GABA and glycine. First, we did not observe GABA_AR-mediated eIPSCs or mIPSCs in mouse LSO neurons (Figs 1 and 3). Such corelease can occur in other systems (see Introduction), and synaptic release can lead to activation of extrasynaptic GABA_BRs elsewhere (Vaaga *et al.* 2014; Tritsch *et al.* 2016). However, we saw no GABA_AR activation upon stimulating MNTB–LSO synapses. Second, our immunohistochemical results show codistribution of gephyrin with GlyT2, but not with GAD65/67 (Fig. 4). The latter finding is supportive of an absence of GABA from presynaptic terminals, including terminals of MNTB axons (see, however, Weisz *et al.* 2016). Double immunolabelling for GAD65/67 and GlyT2 may directly address codistribution of both proteins in a given presynaptic terminal. Preliminary data from our group show a mixed phenotype, namely GlyT2 plus GAD65/67

immunosignals, in only 4% of boutons contacting somata of LSO principal cells in P12 mice (Hirtz *et al.* 2012). Whether the ratio is higher at younger ages needs to be determined.

In the gerbil LSO, immunohistochemical labelling for GABA is medium to intense between P4 and P21 in boutons contacting principal cells (Korada & Schwartz, 1999). Staining for GABA_AR subunits β_2 and β_3 , however, decreases from intense at P4 to light at P14. These data indicate that axon boutons may release GABA onto gerbil LSO neurons throughout development, whereas *synaptic* GABA_AR signalling declines with age. In conclusion, extrasynaptic GABAergic transmission may prevail at older ages in this species as well.

Aside from MNTB axon terminals, another GABA source may be LSO neurons themselves. We found GAD65/67 immunosignals within their somata (Fig. 4), confirming previous reports of GABAergic LSO neurons in rodents (Moore & Moore, 1987; Helfert *et al.* 1989; Korada & Schwartz, 1999; Jenkins & Simmons, 2006). This immunoreactivity is also consistent with vesicular release of GABA from axon terminals in the various target nuclei of LSO neurons. Retrograde GABA release from LSO neurons during spiking activity and subsequent modulation of synaptic input strength has been demonstrated in juvenile gerbils (Magnusson *et al.* 2008). It is unknown whether GABAergic LSO neurons have axon collaterals that terminate in the LSO, either on neighbouring neurons or through autaptic feedback, as shown in the superior paraolivary nucleus adjacent to the LSO (Pollak *et al.* 2011). However, preliminary results in rats indicate that intra-nuclear synaptic connections between LSO neurons are absent (Kim & Kandler, 2003).

Effects of extrasynaptic GABA

Low ambient GABA levels at extrasynaptic GABA_AR sites and a concomitant activation of uninterrupted, tonic conductances occur in many CNS areas (Yeung *et al.* 2003; Semyanov *et al.* 2004). Likewise, tonic GABA conductances are increasingly recognized as important regulators of cell and neuronal network excitability (Glykys & Mody, 2007a; Patel *et al.* 2016), and a multitude of neurological disorders are associated with imbalanced tonic inhibition (Belelli *et al.* 2009; Cope *et al.* 2009; Clarkson *et al.* 2010; Brickley & Mody, 2012; Wu *et al.* 2014). GABA levels can briefly exceed 1 mM at synaptic sites (Cherubini & Conti, 2001; Patel *et al.* 2016). Extrasynaptic GABA concentrations, however, are likely to be in the 10 nM to a few micromolar range (Lerma *et al.* 1986; Attwell *et al.* 1993; Juhasz *et al.* 1997; Maex & De Schutter, 1998; Huang *et al.* 2008; Dvorchak *et al.* 2010; Morishima *et al.* 2010; Karim *et al.* 2012; Numata *et al.* 2012). Thus, the GABA concentrations used in the present study that were sufficient to successfully

elicit tonic responses were probably more than 100-fold lower than they are at synaptic sites (1–10 μ M; Figs 11 and 12). Furthermore, we argue that ambient GABA concentrations are very low in the LSO in a synaptically silent slice preparation (nanomolar range), too low to enable the recording of tonic inhibition. Concentrations rise above detection level only during spike activity (see Glykys & Mody, 2007b; Tang *et al.* 2011). Consequently, constitutively active GABAergic inputs to the LSO appear to be absent *in vitro*. The assumption is consistent with previous reports demonstrating a dependency of ambient GABA levels on neuronal activity (Lerma *et al.* 1986; Rowley *et al.* 1995; Kennedy *et al.* 2002; de Groote & Linthorst, 2007; Vanini *et al.* 2011). Because of the activity dependency, measuring ambient GABA is challenging, and the diversity of experimental conditions and analytical methods makes comparisons of tonic inhibition between studies quite difficult (Bright & Smart, 2013; Christensen *et al.* 2014).

A common thought is that α_{1-3} subunits of GABA_ARs are localized at synapses and mediate phasic inhibition, whereas α_{4-6} subunits are prevalent outside the synapse and mediate tonic inhibition (Karim *et al.* 2012). Our mRNA profiling analysis in the LSO identified 13 transcripts encoding for GABA_AR subunits (Fig. 9). Although some of them, e.g. α_3 and β_3 (position 5 and 8), are typically associated with synaptic-type $\alpha_3\beta_3\gamma_2$ -GABA_ARs (Mortensen *et al.* 2012), α_3 and β_3 can as well combine into binary extrasynaptic $\alpha_3\beta_3$ -GABA_ARs (Mortensen *et al.* 2012). Likewise, α_1 and β_2 subunits (position 9 and 11), which are often compounds of ternary synaptic receptors ($\alpha_1\beta_1\gamma_2$, $\alpha_1\beta_2\gamma_2$, $\alpha_1\beta_3\gamma_2$), can as well coassemble in binary extrasynaptic $\alpha_1\beta_2$ - or ternary extrasynaptic $\alpha_1\beta_2\delta$ -GABA_ARs. In general, GABA is less potent on ternary GABA_ARs ($\alpha_{1-6}\beta_{1-3}\gamma_2$) than on those with binary combinations ($\alpha_{1-6}\beta_{1-3}$; (Ducic *et al.* 1995). We also identified transcripts for the γ_1 and γ_2 subunits (position 7 and 3). γ subunits preferentially coassemble with α_4 and α_6 subunits and predominate at peri- and extrasynaptic locations (Wei *et al.* 2003). The marginal desensitization associated with such receptors makes them ideal for being activated by ambient GABA levels (Mody, 2001), and indeed, $\alpha_6\gamma_2$ -containing receptors were shown to be most sensitive to GABA (Karim *et al.* 2013).

To our knowledge, the α_2 subunit is not associated with extrasynaptic GABA_ARs, but rather restricted to synaptic ones ($\alpha_2\beta_3\gamma_2$). Remarkably, α_2 transcripts were relatively abundant in the LSO (position 6). Our explanation for this surprising result is that α_2 subunits may contribute to synaptic GABA_ARs on non-principal LSO cells, for example lateral olivo-cochlear neurons. Mouse lateral olivo-cochlear neurons receive inhibitory input that is blocked by bicuculline and strychnine (Archakov *et al.* 2003; Sterenborg *et al.* 2010). The slow kinetics of this input are consistent with a GABAergic character.

Some of the most abundant extrasynaptic GABA_ARs are composed of $\alpha_4\beta\delta$ and $\alpha_6\beta\delta$ subunits (Farrant & Nusser, 2005; Jia *et al.* 2005; Beelli *et al.* 2009). Moreover, there is evidence for extrasynaptic $\alpha_4\beta$ - and $\alpha_6\beta$ -GABA_ARs (Bencsits *et al.* 1999; Sinkkonen *et al.* 2004). Our RNA sequencing results are in harmony with the idea of an extrasynaptic location (α_4 position 10, α_6 position 12, δ position 2). Notably, GABA has the highest potency at α_6 -containing receptors and the lowest at α_2 - and α_3 -containing ones, in accordance with low GABA concentrations at extrasynaptic receptor sites (Mortensen *et al.* 2012). As the range of potency is of paramount importance for the activation of GABA_ARs, it affects the role these receptors play in controlling excitability.

Notably, our RNA sequencing analysis identified transcripts for the $\rho 2$ subunit, albeit at a low level (position 13). ρ subunits assemble into ionotropic homomeric receptors originally named GABA_CRs, but after reclassification they are seen as a specialized set of GABA_ARs often referred to as GABA_A- ρ receptors (Naffaa *et al.* 2017). GABA_A- ρ receptors are insensitive to GABA_AR modulators like benzodiazepines, barbiturates and steroids (Bormann & Feigenspan, 1995; Bormann, 2000). Moreover, GABA's potency at homomeric GABA_A- ρ receptors is 10- to 100-fold higher than at heteromeric GABA_ARs, with slow activation and deactivation and less desensitization (Bormann & Feigenspan, 1995; Bormann, 2000). Again, these features are hallmarks of extrasynaptic receptors. Interestingly, and of some relevance for pharmacological experiments with THIP, besides being an agonist at δ -GABA_ARs, THIP is also a GABA_A- ρ receptor antagonist (Johnston *et al.* 2003). Collectively, with the exception of the α_1 subunit, all subunits identified via transcript profiling can be a component of extrasynaptic GABA_ARs. Many open issues remain concerning the abundance, composition and function of extrasynaptic GABA_ARs in the LSO, and these issues require future research, including very high-resolution studies of gene expression patterns such as single-cell RNA sequencing (Patch-seq; Cadwell *et al.* 2016).

Tonic activation of extrasynaptic GABA_ARs regulates neuronal excitability (Otis *et al.* 1991; Salin & Prince, 1996; Bautista *et al.* 2010), yet the impact varies across brain region and cell type (Lee & Maguire, 2014). Moreover, tonic activation does not necessarily imply tonic inhibition and spike suppression. With relatively positive Cl^- reversal potentials ($E_{\text{Cl}^-} > V_{\text{M}}$) and a strong enough conductance, the action of high-affinity extrasynaptic GABA_ARs may be excitatory (Song *et al.* 2011; Bright & Smart, 2013). Indeed, increased excitability has been described upon tonic activation of GABA_ARs (Kilb *et al.* 2013; Yu *et al.* 2013). Our findings of persistent hyperpolarizing or depolarizing effects when patch pipettes were filled with 2 mM or 32 mM $[\text{Cl}^-]$, respectively, are in full agreement with this conclusion (Figs 11 and 12). By controlling developmental

activity patterns in the prenatal and neonatal brain, the modulatory role of GABA appears to be closely associated with the formation of neuronal circuits (Kilb *et al.* 2013).

Conclusions

Our results imply that mouse MNTB–LSO inputs lack synaptic GABA signalling. Nevertheless, GABA causes pre-synaptic effects on axon terminals of MNTB neurons via GABA_BRs where it reduces activity-evoked Ca^{2+} influx. The lower Ca^{2+} levels will probably reduce transmitter release from axon terminals and thus dampen glycinergic transmission in the MNTB–LSO projection. Moreover, GABA causes postsynaptic effects on LSO principal neurons via extrasynaptic GABA_ARs likely to contain α_5 and δ subunits. Extrasynaptic GABA signalling increases the excitability and facilitates spike generation in immature LSO neurons, which have a high $[\text{Cl}^-]_{\text{i}}$. In contrast, it decreases the excitability in mature neurons, which have a low $[\text{Cl}^-]_{\text{i}}$, and thereby suppresses spike generation. Collectively, we conclude that GABA is a modulatory transmitter in the mouse LSO rather than playing a direct role in fast inhibitory neurotransmission. Because of the multitude of GABA receptor subunits, GABA appears to be in a better position to function as a modulator than glycine, which acts on receptors of relatively uniform nature. Whether the scenario is also present in other species or unique to the mouse MNTB–LSO circuit needs to be determined.

References

- Abdi H (2007). The Bonferonni and Šidák corrections for multiple comparisons. In *Encyclopedia of Measurement and Statistics*, ed. Salkind E, pp. 103–107. Sage, Thousand Oaks.
- Alexander SP, Kelly E, Marrion NV, Peters JA, Faccenda E, Harding SD, Pawson AJ, Sharman JL, Southan C, Davies JA & Collaborators C (2017). The concise guide to pharmacology 2017/18: Transporters. *Br J Pharmacol* **174**(Suppl 1), S360–S446.
- Apostolides PF & Trussell LO (2013). Rapid, activity-independent turnover of vesicular transmitter content at a mixed glycine/GABA synapse. *J Neurosci* **33**, 4768–4781.
- Archakov AI, Govorun VM, Dubanov AV, Ivanov YD, Veselovsky AV, Lewi P & Janssen P (2003). Protein-protein interactions as a target for drugs in proteomics. *Proteomics* **3**, 380–391.
- Attwell D, Barbour B & Szatkowski M (1993). Nonvesicular release of neurotransmitter. *Neuron* **11**, 401–407.
- Awatramani GB, Turecek R & Trussell LO (2005). Staggered development of GABAergic and glycinergic transmission in the MNTB. *J Neurophysiol* **93**, 819–828.
- Balakrishnan V, Becker M, Löhrike S, Nothwang HG, Güresir E & Friauf E (2003). Expression and function of chloride transporters during development of inhibitory

- neurotransmission in the auditory brainstem. *J Neurosci* **23**, 4134–4145.
- Barbour B & Häusser M (1997). Intersynaptic diffusion of neurotransmitter. *Trends Neurosci* **20**, 377–384.
- Bautista W, Aguilar J, Loeza-Alcocer JE & Delgado-Lezama R (2010). Pre- and postsynaptic modulation of monosynaptic reflex by GABA_A receptors on turtle spinal cord. *J Physiol* **588**, 2621–2631.
- Beato M, Burzomato V & Sivilotti LG (2007). The kinetics of inhibition of rat recombinant heteromeric $\alpha 1\beta$ glycine receptors by the low-affinity antagonist SR-95531. *J Physiol* **580**, 171–179.
- Becker CM, Hoch W & Betz H (1988). Glycine receptor heterogeneity in rat spinal cord during postnatal development. *EMBO J* **7**, 3717–3726.
- Bekkers JM (2005). Presynaptically silent GABA synapses in hippocampus. *J Neurosci* **25**, 4031–4039.
- Belelli D, Harrison NL, Maguire J, Macdonald RL, Walker MC & Cope DW (2009). Extrasynaptic GABA_A receptors: form, pharmacology, and function. *J Neurosci* **29**, 12757–12763.
- Bencsits E, Ebert V, Tretter V & Sieghart W (1999). A significant part of native γ -aminobutyric acid_A receptors containing α_4 subunits do not contain γ or δ subunits. *J Biol Chem* **274**, 19613–19616.
- Betz H & Laube B (2006). Glycine receptors: recent insights into their structural organization and functional diversity. *J Neurochem* **97**, 1600–1610.
- Bolte S & Cordelieres FP (2006). A guided tour into subcellular colocalization analysis in light microscopy. *J Microsc* **224**, 213–232.
- Bormann J (2000). The ‘ABC’ of GABA receptors. *Trends Pharmacol Sci* **21**, 16–19.
- Bormann J & Feigenspan A (1995). GABA_C receptors. *Trends Neurosci* **18**, 515–519.
- Brenowitz S, David J & Trussell L (1998). Enhancement of synaptic efficacy by presynaptic GABA_B receptors. *Neuron* **20**, 135–141.
- Brickley SG, Cull-Candy SG & Farrant M (1999). Single-channel properties of synaptic and extrasynaptic GABA_A receptors suggest differential targeting of receptor subtypes. *J Neurosci* **19**, 2960–2973.
- Brickley SG & Mody I (2012). Extrasynaptic GABA_A receptors: their function in the CNS and implications for disease. *Neuron* **73**, 23–34.
- Bright DP & Smart TG (2013). Methods for recording and measuring tonic GABA_A receptor-mediated inhibition. *Front Neural Circuits* **7**, 193.
- Brown N, Kerby J, Bonnert TP, Whiting PJ & Wafford KA (2002). Pharmacological characterization of a novel cell line expressing human $\alpha_4\beta_3\delta$ GABA_A receptors. *Br J Pharmacol* **136**, 965–974.
- Cadwell CR, Palasantza A, Jiang X, Berens P, Deng Q, Yilmaz M, Reimer J, Shen S, Bethge M, Tolias KF, Sandberg R & Tolias AS (2016). Electrophysiological, transcriptomic and morphologic profiling of single neurons using Patch-seq. *Nat Biotechnol* **34**, 199–203.
- Caspary DM & Finlayson PG (1991). Superior olivary complex: Functional neuropharmacology of the principal cell types. In *Neurobiology of Hearing: The Central Auditory System*, ed. Altschuler RA, Bobbin RP, Clopton BM & Hoffman DW, pp. 141–161. Raven Press, New York.
- Chanda S, Oh S & Xu-Friedman MA (2011). Calcium imaging of auditory nerve fiber terminals in the cochlear nucleus. *J Neurosci Methods* **195**, 24–29.
- Charpier S, Behrends JC, Triller A, Faber DS & Korn H (1995). ‘Latent’ inhibitory connections become functional during activity-dependent plasticity. *Proc Natl Acad Sci U S A* **92**, 117–120.
- Cherubini E & Conti F (2001). Generating diversity at GABAergic synapses. *Trends Neurosci* **24**, 155–162.
- Christensen RK, Petersen AV, Schmitt N & Perrier JF (2014). Fast detection of extrasynaptic GABA with a whole-cell sniffer. *Front Cell Neurosci* **8**, 133.
- Clarkson AN, Huang BS, Macisaac SE, Mody I & Carmichael ST (2010). Reducing excessive GABA-mediated tonic inhibition promotes functional recovery after stroke. *Nature* **468**, 305–309.
- Cope DW, Di Giovanni G, Fyson SJ, Orban G, Errington AC, Lorincz ML, Gould TM, Carter DA & Crunelli V (2009). Enhanced tonic GABA_A inhibition in typical absence epilepsy. *Nat Med* **15**, 1392–1398.
- Crook J, Hendrickson A & Robinson FR (2006). Co-localization of glycine and GABA immunoreactivity in interneurons in *Macaca* monkey cerebellar cortex. *Neuroscience* **141**, 1951–1959.
- Dalby NO (2000). GABA-level increasing and convulsive effects of three different GABA uptake inhibitors. *Neuropharmacology* **39**, e2399–e2407.
- de Groote L & Linthorst AC (2007). Exposure to novelty and forced swimming evoke stressor-dependent changes in extracellular GABA in the rat hippocampus. *Neuroscience* **148**, 773–782.
- Dittman JS & Regehr WG (1996). Contributions of calcium-dependent and calcium-independent mechanisms to presynaptic inhibition at a cerebellar synapse. *J Neurosci* **16**, 1623–1633.
- Dobin A & Gingeras TR (2015). Mapping RNA-seq reads with STAR. *Curr Protoc Bioinformatics* **51**, 11.14.11–19.
- Drasbek KR & Jensen K (2006). THIP, a hypnotic and antinociceptive drug, enhances an extrasynaptic GABA_A receptor-mediated conductance in mouse neocortex. *Cereb Cortex* **16**, 1134–1141.
- Ducic I, Caruncho HJ, Zhu WJ, Vicini S & Costa E (1995). γ -Aminobutyric acid gating of Cl⁻ channels in recombinant GABA_A receptors. *J Pharmacol Exp Ther* **272**, 438–445.
- Dufour A, Tell F & Baude A (2010). Perinatal development of inhibitory synapses in the nucleus tractus solitarii of the rat. *Eur J Neurosci* **32**, 538–549.
- Dugué GP, Dumoulin A, Triller A & Dieudonné S (2005). Target-dependent use of co-released inhibitory transmitters at central synapses. *J Neurosci* **25**, 6490–6498.
- Dumoulin A, Triller A & Dieudonné S (2001). IPSC kinetics at identified GABAergic and mixed GABAergic and glycinergic synapses onto cerebellar Golgi cells. *J Neurosci* **21**, 6045–6057.
- Dvorzhak A, Myakhar O, Unichenko P, Kirmse K & Kirischuk S (2010). Estimation of ambient GABA levels in layer I of the mouse neonatal cortex in brain slices. *J Physiol* **588**, 2351–2360.

- Ehrlich I, Löhrlke S & Friauf E (1999). Shift from depolarizing to hyperpolarizing glycine action in rat auditory neurons is due to age-dependent Cl^- regulation. *J Physiol* **520**, 121–137.
- Eulenburg V, Armsen W, Betz H & Gomeza J (2005). Glycine transporters: essential regulators of neurotransmission. *Trends Biochem Sci* **30**, 325–333.
- Farrant M & Nusser Z (2005). Variations on an inhibitory theme: phasic and tonic activation of GABA_A receptors. *Nat Rev Neurosci* **6**, 215–229.
- Friauf E, Aragon C, Löhrlke S, Westenfelder B & Zafra F (1999). Developmental expression of the glycine transporter GLYT2 in the auditory system of rats suggests involvement in synapse maturation. *J Comp Neurol* **412**, 17–37.
- Friauf E, Fischer AU & Fuhr MF (2015). Synaptic plasticity in the auditory system: a review. *Cell Tissue Res* **361**, 177–213.
- Friauf E, Hammerschmidt B & Kirsch J (1997). Development of adult-type inhibitory glycine receptors in the central auditory system of rats. *J Comp Neurol* **385**, 117–134.
- Gassmann M & Bettler B (2012). Regulation of neuronal GABA_B receptor functions by subunit composition. *Nat Rev Neurosci* **13**, 380–394.
- Ghavanini AA, Mathers DA, Kim HS & Puil E (2006). Distinctive glycinergic currents with fast and slow kinetics in thalamus. *J Neurophysiol* **95**, 3438–3448.
- Giugovaz-Tropper B, Gonzalez-Inchauspe C, Di Guilmi MN, Urbano FJ, Forsythe ID & Uchitel OD (2011). P/Q-type calcium channel ablation in a mice glycinergic synapse mediated by multiple types of Ca^{2+} channels alters transmitter release and short term plasticity. *Neuroscience* **192**, 219–230.
- Glykys J, Mann EO & Mody I (2008). Which GABA_A receptor subunits are necessary for tonic inhibition in the hippocampus? *J Neurosci* **28**, 1421–1426.
- Glykys J & Mody I (2007a). Activation of GABA_A receptors: views from outside the synaptic cleft. *Neuron* **56**, 763–770.
- Glykys J & Mody I (2007b). The main source of ambient GABA responsible for tonic inhibition in the mouse hippocampus. *J Physiol* **582**, 1163–1178.
- Grothe B & Pecka M (2014). The natural history of sound localization in mammals – a story of neuronal inhibition. *Front Neural Circuits* **8**, 116.
- Grundy D (2015). Principles and standards for reporting animal experiments in *The Journal of Physiology* and *Experimental Physiology*. *J Physiol* **593**, 2547–2549.
- Gundersen V, Storm-Mathisen J & Bergersen LH (2015). Neuroglial transmission. *Physiol Rev* **95**, 695–726.
- Heja L, Barabas P, Nyitrai G, Kekesi KA, Lasztocki B, Toke O, Tarkanyi G, Madsen K, Schousboe A, Dobolyi A, Palkovits M & Kardos J (2009). Glutamate uptake triggers transporter-mediated GABA release from astrocytes. *PLoS One* **4**, e7153.
- Helfert RH, Bonneau JM, Wenthold RJ & Altschuler RA (1989). GABA and glycine immunoreactivity in the guinea pig superior olivary complex. *Brain Res* **501**, 269–286.
- Hirtz JJ, Braun N, Griesemer D, Hannes C, Janz K, Löhrlke S, Müller B & Friauf E (2012). Synaptic refinement of an inhibitory topographic map in the auditory brainstem requires functional $\text{Ca}_v1.3$ calcium channels. *J Neurosci* **32**, 14602–14616.
- Hnasko TS & Edwards RH (2012). Neurotransmitter corelease: mechanism and physiological role. *Annu Rev Physiol* **74**, 225–243.
- Hoestgaard-Jensen K, Dalby NO, Krall J, Hammer H, Krogsgaard-Larsen P, Frølund B & Jensen AA (2014). Probing $\alpha_4\beta\delta$ GABA_A receptor heterogeneity: differential regional effects of a functionally selective $\alpha_4\beta_1\delta/\alpha_4\beta_3\delta$ receptor agonist on tonic and phasic inhibition in rat brain. *J Neurosci* **34**, 16256–16272.
- Huang M, Li Z, Dai J, Shahid M, Wong EH & Meltzer HY (2008). Asenapine increases dopamine, norepinephrine, and acetylcholine efflux in the rat medial prefrontal cortex and hippocampus. *Neuropsychopharmacology* **33**, 2934–2945.
- Ishibashi H, Yamaguchi J, Nakahata Y & Nabekura J (2013). Dynamic regulation of glycine–GABA co-transmission at spinal inhibitory synapses by neuronal glutamate transporter. *J Physiol* **591**, 3821–3832.
- Jenkins SA & Simmons DD (2006). GABAergic neurons in the lateral superior olive of the hamster are distinguished by differential expression of gad isoforms during development. *Brain Res* **1111**, 12–25.
- Jia F, Pignataro L, Schofield CM, Yue M, Harrison NL & Goldstein PA (2005). An extrasynaptic GABA_A receptor mediates tonic inhibition in thalamic VB neurons. *J Neurophysiol* **94**, 4491–4501.
- Johnston GA, Chebib M, Hanrahan JR & Mewett KN (2003). GABA_C receptors as drug targets. *Curr Drug Targets CNS Neurol Disord* **2**, 260–268.
- Jonas P, Bischofberger J & Sandkühler J (1998). Corelease of two fast neurotransmitters at a central synapse. *Science* **281**, 419–424.
- Jones MV & Westbrook GL (1995). Desensitized states prolong GABA_A channel responses to brief agonist pulses. *Neuron* **15**, 181–191.
- Juhasz G, Kekesi KA, Nyitrai G, Dobolyi A, Krogsgaard-Larsen P & Schousboe A (1997). Differential effects of nipecotic acid and 4,5,6,7-tetrahydroisoxazolo[4,5-c]pyridin-3-ol on extracellular gamma-aminobutyrate levels in rat thalamus. *Eur J Pharmacol* **331**, 139–144.
- Kandler K & Friauf E (1995). Development of glycinergic and glutamatergic synaptic transmission in the auditory brainstem of perinatal rats. *J Neurosci* **15**, 6890–6904.
- Karim N, Wellendorph P, Absalom N, Bang LH, Jensen ML, Hansen MM, Lee HJ, Johnston GA, Hanrahan JR & Chebib M (2012). Low nanomolar GABA effects at extrasynaptic $\alpha_4\beta_1/\beta_3\delta$ GABA_A receptor subtypes indicate a different binding mode for GABA at these receptors. *Biochem Pharmacol* **84**, 549–557.
- Karim N, Wellendorph P, Absalom N, Johnston GA, Hanrahan JR & Chebib M (2013). Potency of GABA at human recombinant GABA_A receptors expressed in *Xenopus* oocytes: a mini review. *Amino Acids* **44**, 1139–1149.
- Kasyanov AM, Safulina VF, Voronin LL & Cherubini E (2004). GABA-mediated giant depolarizing potentials as coincidence detectors for enhancing synaptic efficacy in the developing hippocampus. *Proc Natl Acad Sci U S A* **101**, 3967–3972.
- Keller AF, Coull JAM, Chéry N, Poisbeau P & De Koninck Y (2001). Region-specific developmental specialization of

- GABA-glycine cosynapses in laminae I-II of the rat spinal dorsal horn. *J Neurosci* **21**, 7871–7880.
- Kennedy RT, Thompson JE & Vickroy TW (2002). In vivo monitoring of amino acids by direct sampling of brain extracellular fluid at ultralow flow rates and capillary electrophoresis. *J Neurosci Methods* **114**, 39–49.
- Keros S & Hablitz JJ (2005). Subtype-specific GABA transporter antagonists synergistically modulate phasic and tonic GABA_A conductances in rat neocortex. *J Neurophysiol* **94**, 2073–2085.
- Kilb W, Kirischuk S & Luhmann HJ (2013). Role of tonic GABAergic currents during pre- and early postnatal rodent development. *Front Neural Circuits* **7**, 139.
- Kim G & Kandler K (2003). Elimination and strengthening of glycinergic/GABAergic connections during tonotopic map formation. *Nat Neurosci* **6**, 282–290.
- Kim G & Kandler K (2010). Synaptic changes underlying the strengthening of GABA/glycinergic connections in the developing lateral superior olive. *Neuroscience* **171**, 924–933.
- Kneussel M & Loeblich S (2007). Trafficking and synaptic anchoring of ionotropic inhibitory neurotransmitter receptors. *Biol Cell* **99**, 297–309.
- Knoflach F, Hernandez MC & Bertrand D (2016). GABA_A receptor-mediated neurotransmission: not so simple after all. *Biochem Pharmacol* **115**, 10–17.
- Korada S & Schwartz IR (1999). Development of GABA, glycine, and their receptors in the auditory brainstem of gerbil: A light and electron microscopic study. *J Comp Neurol* **409**, 664–681.
- Kotak VC, Korada S, Schwartz IR & Sanes DH (1998). A developmental shift from GABAergic to glycinergic transmission in the central auditory system. *J Neurosci* **18**, 4646–4655.
- Krächan EG, Fischer AU, Franke J & Friauf E (2017). Synaptic reliability and temporal precision are achieved via high quantal content and effective replenishment: auditory brainstem versus hippocampus. *J Physiol* **595**, 839–864.
- Kramer F, Griesemer D, Bakker D, Brill S, Franke J, Frotscher E & Friauf E (2014). Inhibitory glycinergic neurotransmission in the mammalian auditory brainstem upon prolonged stimulation: short-term plasticity and synaptic reliability. *Front Neural Circuits* **8**, 14.
- Krogsgaard-Larsen P, Frølund B, Jørgensen FS & Schousboe A (1994). GABA_A receptor agonists, partial agonists, and antagonists: design and therapeutic prospects. *J Med Chem* **37**, 2489–2505.
- Krogsgaard-Larsen P, Frølund B & Liljefors T (2002). Specific GABA_A agonists and partial agonists. *Chem Rec* **2**, 419–430.
- Krogsgaard-Larsen P, Frølund B, Liljefors T & Ebert B (2004). GABA_A agonists and partial agonists: THIP (Gaboxadol) as a non-opioid analgesic and a novel type of hypnotic. *Biochem Pharmacol* **68**, 1573–1580.
- Kungel M & Friauf E (1997). Physiology and pharmacology of native glycine receptors in developing rat auditory brainstem neurons. *Brain Res Dev Brain Res* **102**, 157–165.
- Lee V & Maguire J (2014). The impact of tonic GABA_A receptor-mediated inhibition on neuronal excitability varies across brain region and cell type. *Front Neural Circuits* **8**, 3.
- Leira J, Herranz AS, Herreras O, Abaira V & Martin del Rio R (1986). In vivo determination of extracellular concentration of amino acids in the rat hippocampus. A method based on brain dialysis and computerized analysis. *Brain Res* **384**, 145–155.
- Li P & Slaughter M (2007). Glycine receptor subunit composition alters the action of GABA antagonists. *Vis Neurosci* **24**, 513–521.
- Liao Y, Smyth GK & Shi W (2014). featureCounts: an efficient general purpose program for assigning sequence reads to genomic features. *Bioinformatics* **30**, 923–930.
- Löhrke S, Srinivasan G, Oberhofer M, Doncheva E & Friauf E (2005). Shift from depolarizing to hyperpolarizing glycine action occurs at different perinatal ages in superior olivary complex nuclei. *Eur J Neurosci* **22**, 2708–2722.
- Lüscher C & Slesinger PA (2010). Emerging roles for G protein-gated inwardly rectifying potassium (GIRK) channels in health and disease. *Nat Rev Neurosci* **11**, 301–315.
- Lynch JW (2004). Molecular structure and function of the glycine receptor chloride channel. *Physiol Rev* **84**, 1051–1095.
- Lynch JW (2009). Native glycine receptor subtypes and their physiological roles. *Neuropharmacology* **56**, 303–309.
- Madsen KK, White HS & Schousboe A (2010). Neuronal and non-neuronal GABA transporters as targets for antiepileptic drugs. *Pharmacol Ther* **125**, 394–401.
- Maex R & De Schutter E (1998). Synchronization of Golgi and granule cell firing in a detailed network model of the cerebellar granule cell layer. *J Neurophysiol* **80**, 2521–2537.
- Magnusson AK, Park TJ, Pecka M, Grothe B & Koch U (2008). Retrograde GABA signaling adjusts sound localization by balancing excitation and inhibition in the brainstem. *Neuron* **59**, 125–137.
- Meera P, Wallner M & Otis TS (2011). Molecular basis for the high THIP/gaboxadol sensitivity of extrasynaptic GABA_A receptors. *J Neurophysiol* **106**, 2057–2064.
- Mody I (2001). Distinguishing between GABA_A receptors responsible for tonic and phasic conductances. *Neurochem Res* **26**, 907–913.
- Mody I (2005). Aspects of the homeostatic plasticity of GABA_A receptor-mediated inhibition. *J Physiol* **562**, 37–46.
- Moore JK & Moore RY (1987). Glutamic acid decarboxylase-like immunoreactivity in brainstem auditory nuclei of the rat. *J Comp Neurol* **260**, 157–174.
- Moore LA & Trussell LO (2017). Corelease of inhibitory neurotransmitters in the mouse auditory midbrain. *J Neurosci* **37**, 9453–9464.
- Morishima T, Uematsu M, Furukawa T, Yanagawa Y, Fukuda A & Yoshida S (2010). GABA imaging in brain slices using immobilized enzyme-linked photoanalysis. *Neurosci Res* **67**, 347–353.
- Mortensen M, Ebert B, Wafford K & Smart TG (2010). Distinct activities of GABA agonists at synaptic- and extrasynaptic-type GABA_A receptors. *J Physiol* **588**, 1251–1268.
- Mortensen M, Patel B & Smart TG (2012). GABA potency at GABA_A receptors found in synaptic and extrasynaptic zones. *Front Cell Neurosci* **6**, 1.
- Muller E, Le Corrionc H, Triller A & Legendre P (2006). Developmental dissociation of presynaptic inhibitory

- neurotransmitter and postsynaptic receptor clustering in the hypoglossal nucleus. *Mol Cell Neurosci* **32**, 254–273.
- Nabekura J, Katsurabayashi S, Kakazu Y, Shibata S, Matsubara A, Jinno S, Mizoguchi Y, Sasaki A & Ishibashi H (2004). Developmental switch from GABA to glycine release in single central synaptic terminals. *Nat Neurosci* **7**, 17–23.
- Naffaa MM, Hung S, Chebib M, Johnston GAR & Hanrahan JR (2017). GABA- ρ receptors: distinctive functions and molecular pharmacology. *Br J Pharmacol* **174**, 1881–1894.
- Nerlich J, Kuenzel T, Keine C, Korenic A, Rübnsamen R & Milenkovic I (2014). Dynamic fidelity control to the central auditory system: synergistic glycine/GABAergic inhibition in the cochlear nucleus. *J Neurosci* **34**, 11604–11620.
- Nerlich J, Rübnsamen R & Milenkovic I (2017). Developmental shift of inhibitory transmitter content at a central auditory synapse. *Front Cell Neurosci* **11**, 211.
- Numata JM, van Brederode JF & Berger AJ (2012). Lack of an endogenous GABA_A receptor-mediated tonic current in hypoglossal motoneurons. *J Physiol* **590**, 2965–2976.
- O'Brien JA & Berger AJ (1999). Cotransmission of GABA and glycine to brain stem motoneurons. *J Neurophysiol* **82**, 1638.
- Olsen RW & Sieghart W (2008). International Union of Pharmacology. LXX. Subtypes of gamma-aminobutyric acid_A receptors: classification on the basis of subunit composition, pharmacology, and function. Update. *Pharmacol Rev* **60**, 243–260.
- Orser BA (2006). Extrasynaptic GABA_A receptors are critical targets for sedative-hypnotic drugs. *J Clin Sleep Med* **2**, S12–18.
- Otis TS, Staley KJ & Mody I (1991). Perpetual inhibitory activity in mammalian brain slices generated by spontaneous GABA release. *Brain Res* **545**, 142–150.
- Ottersen OP, Storm-Mathisen J & Somogyi P (1988). Colocalization of glycine-like and GABA-like immunoreactivities in Golgi cell terminals in the rat cerebellum: a postembedding light and electron microscopic study. *Brain Res* **450**, 342–353.
- Patel B, Bright DP, Mortensen M, Frølund B & Smart TG (2016). Context-dependent modulation of GABA_AR-mediated tonic currents. *J Neurosci* **36**, 607–621.
- Picelli S, Bjorklund AK, Faridani OR, Sagasser S, Winberg G & Sandberg R (2013). Smart-seq2 for sensitive full-length transcriptome profiling in single cells. *Nat Methods* **10**, 1096–1098.
- Piechotta K, Weth F, Harvey RJ & Friauf E (2001). Localization of rat glycine receptor $\alpha 1$ and $\alpha 2$ subunit transcripts in the developing auditory brainstem. *J Comp Neurol* **438**, 336–352.
- Pilati N, Linley DM, Selvaskandan H, Uchitel O, Hennig MH, Kopp-Scheinflug C & Forsythe ID (2016). Acoustic trauma slows AMPA receptor-mediated EPSCs in the auditory brainstem, reducing GluA4 subunit expression as a mechanism to rescue binaural function. *J Physiol* **594**, 3683–3703.
- Pollak GD, Gittelman JX, Li N & Xie RL (2011). Inhibitory projections from the ventral nucleus of the lateral lemniscus and superior paraolivary nucleus create directional selectivity of frequency modulations in the inferior colliculus: A comparison of bats with other mammals. *Hear Res* **273**, 134–144.
- Rahman J, Latal AT, Besser S, Hirrlinger J & Hülsmann S (2013). Mixed miniature postsynaptic currents resulting from co-release of glycine and GABA recorded from glycinergic neurons in the neonatal respiratory network. *Eur J Neurosci* **37**, 1229–1241.
- Ramakrishnan NA, Drescher MJ, Morley BJ, Kelley PM & Drescher DG (2014). Calcium regulates molecular interactions of otoferlin with soluble NSF attachment protein receptor (SNARE) proteins required for hair cell exocytosis. *J Biol Chem* **289**, 8750–8766.
- Regehr WG & Atluri PP (1995). Calcium transients in cerebellar granule cell presynaptic terminals. *Biophys J* **68**, 2156–2170.
- Richerson GB & Wu Y (2003). Dynamic equilibrium of neurotransmitter transporters: not just for reuptake anymore. *J Neurophysiol* **90**, 1363–1374.
- Rowley HL, Martin KF & Marsden CA (1995). Determination of in vivo amino acid neurotransmitters by high-performance liquid chromatography with *o*-phthalaldehyde-sulphite derivatisation. *J Neurosci Methods* **57**, 93–99.
- Rudolph U & Möhler H (2014). GABA_A receptor subtypes: therapeutic potential in Down syndrome, affective disorders, schizophrenia, and autism. *Annu Rev Pharmacol Toxicol* **54**, 483–507.
- Russier M, Kopysova IL, Ankri N, Ferrand N & Debanne D (2002). GABA and glycine co-release optimizes functional inhibition in rat brainstem motoneurons *in vitro*. *J Physiol* **541**, 123–137.
- Salin PA & Prince DA (1996). Spontaneous GABA_A receptor-mediated inhibitory currents in adult rat somatosensory cortex. *J Neurophysiol* **75**, 1573–1588.
- Sanes DH (1993). The development of synaptic function and integration in the central auditory system. *J Neurosci* **13**, 2627–2637.
- Schindelin J, Arganda-Carreras I, Frise E, Kaynig V, Longair M, Pietzsch T, Preibisch S, Rueden C, Saalfeld S, Schmid B, Tinevez JY, White DJ, Hartenstein V, Eliceiri K, Tomancak P & Cardona A (2012). Fiji: an open-source platform for biological-image analysis. *Nat Methods* **9**, 676–682.
- Schwenk J, Perez-Garci E, Schneider A, Kollwe A, Gauthier-Kemper A, Fritzius T, Raveh A, Dinamarca MC, Hanuschkin A, Bildl W, Klingauf J, Gassmann M, Schulte U, Bettler B & Fakler B (2016). Modular composition and dynamics of native GABA_B receptors identified by high-resolution proteomics. *Nat Neurosci* **19**, 233–242.
- Semyanov A, Walker MC, Kullmann DM & Silver RA (2004). Tonically active GABA_A receptors: modulating gain and maintaining the tone. *Trends Neurosci* **27**, 262–269.
- Singer JH, Talley EM, Bayliss DA & Berger AJ (1998). Development of glycinergic synaptic transmission to rat brain stem motoneurons. *J Neurophysiol* **80**, 2608–2620.
- Sinkkonen ST, Vekovischeva OY, Moykkynen T, Ogris W, Sieghart W, Wisden W & Korpi ER (2004). Behavioural correlates of an altered balance between synaptic and extrasynaptic GABA_Aergic inhibition in a mouse model. *Eur J Neurosci* **20**, 2168–2178.
- Smart TG (2015). GABA_A receptors. In *Handbook of Ion Channels*, ed. Zheng J & Trudeau MC, pp. 345–359. CRC, Boca Raton, FL.

- Smart TG & Paoletti P (2012). Synaptic neurotransmitter-gated receptors. *Cold Spring Harb Perspect Biol* **4**, a009662.
- Song I, Savtchenko L & Semyanov A (2011). Tonic excitation or inhibition is set by GABA_A conductance in hippocampal interneurons. *Nat Commun* **2**, 376.
- Specht CG, Izeddin I, Rodriguez PC, El Beheiry M, Rostaing P, Darzacq X, Dahan M & Triller A (2013). Quantitative nanoscopy of inhibitory synapses: counting gephyrin molecules and receptor binding sites. *Neuron* **79**, 308–321.
- Stange A, Myoga MH, Lingner A, Ford MC, Alexandrova O, Felmy F, Pecka M, Siveke I & Grothe B (2013). Adaptation in sound localization: from GABA_B receptor-mediated synaptic modulation to perception. *Nat Neurosci* **16**, 1840–1847.
- Stephan J & Friauf E (2014). Functional analysis of the inhibitory neurotransmitter transporters GlyT1, GAT-1, and GAT-3 in astrocytes of the lateral superior olive. *Glia* **62**, 1992–2003.
- Sterenburg JC, Pilati N, Sheridan CJ, Uchitel OD, Forsythe ID & Barnes-Davies M (2010). Lateral olivocochlear (LOC) neurons of the mouse LSO receive excitatory and inhibitory synaptic inputs with slower kinetics than LSO principal neurons. *Hear Res* **270**, 119–126.
- Takahashi T, Kajikawa Y & Tsujimoto T (1998). G-protein-coupled modulation of presynaptic calcium currents and transmitter release by a GABA_B receptor. *J Neurosci* **18**, 3138–3146.
- Takahashi T, Momiyama A, Hirai K, Hishinuma F & Akagi H (1992). Functional correlation of fetal and adult forms of glycine receptors with developmental changes in inhibitory synaptic receptor channels. *Neuron* **9**, 1155–1161.
- Tang ZQ, Dinh EH, Shi W & Lu Y (2011). Ambient GABA-activated tonic inhibition sharpens auditory coincidence detection via a depolarizing shunting mechanism. *J Neurosci* **31**, 6121–6131.
- Thomas P, Mortensen M, Hosie AM & Smart TG (2005). Dynamic mobility of functional GABA_A receptors at inhibitory synapses. *Nat Neurosci* **8**, 889–897.
- Todd AJ, Watt C, Spike RC & Sieghart W (1996). Colocalization of GABA, glycine, and their receptors at synapses in the rat spinal cord. *J Neurosci* **16**, 974–982.
- Tritsch NX, Granger AJ & Sabatini BL (2016). Mechanisms and functions of GABA co-release. *Nat Rev Neurosci* **17**, 139–145.
- Tyagarajan SK & Fritschy JM (2014). Gephyrin: a master regulator of neuronal function? *Nat Rev Neurosci* **15**, 141–156.
- Unichenko P, Dvorzhak A & Kirischuk S (2013). Transporter-mediated replacement of extracellular glutamate for GABA in the developing murine neocortex. *Eur J Neurosci* **38**, 11.
- Vaaga CE, Borisovska M & Westbrook GL (2014). Dual-transmitter neurons: functional implications of co-release and co-transmission. *Curr Opin Neurobiol* **29**, 25–32.
- Vanini G, Wathen BL, Lydic R & Baghdoyan HA (2011). Endogenous GABA levels in the pontine reticular formation are greater during wakefulness than during rapid eye movement sleep. *J Neurosci* **31**, 2649–2656.
- Walcher J, Hassfurth B, Grothe B & Koch U (2011). Comparative posthearing development of inhibitory inputs to the lateral superior olive in gerbils and mice. *J Neurophysiol* **106**, 1443–1453.
- Walker MC & Semyanov A (2008). Regulation of excitability by extrasynaptic GABA_A receptors. In *Results and Problems in Cell Differentiation*, ed. Darlison MG, pp. 29–48. Springer, Berlin, Heidelberg.
- Wang P & Slaughter MM (2005). Effects of GABA receptor antagonists on retinal glycine receptors and on homomeric glycine receptor alpha subunits. *J Neurophysiol* **93**, 3120–3126.
- Wei W, Zhang N, Peng Z, Houser CR & Mody I (2003). Perisynaptic localization of δ subunit-containing GABA_A receptors and their activation by GABA spillover in the mouse dentate gyrus. *J Neurosci* **23**, 10650–10661.
- Weisz CJ, Rubio ME, Givens RS & Kandler K (2016). Excitation by axon terminal GABA spillover in a sound localization circuit. *J Neurosci* **36**, 911–925.
- Wohlfarth KM, Bianchi MT & Macdonald RL (2002). Enhanced neurosteroid potentiation of ternary GABA_A receptors containing the δ subunit. *J Neurosci* **22**, 1541–1549.
- Wu LG & Saggau P (1995). GABA_B receptor-mediated presynaptic inhibition in guinea-pig hippocampus is caused by reduction of presynaptic Ca²⁺ influx. *J Physiol* **485**, 649–657.
- Wu Z, Guo Z, Gearing M & Chen G (2014). Tonic inhibition in dentate gyrus impairs long-term potentiation and memory in an Alzheimer's disease model. *Nat Commun* **5**, 4159.
- Xu C, Zhang W, Rondard P, Pin JP & Liu J (2014). Complex GABA_B receptor complexes: how to generate multiple functionally distinct units from a single receptor. *Front Pharmacol* **5**, 12.
- Yeung JY, Canning KJ, Zhu G, Pennefather P, MacDonald JF & Orser BA (2003). Tonically activated GABA_A receptors in hippocampal neurons are high-affinity, low-conductance sensors for extracellular GABA. *Mol Pharmacol* **63**, 2–8.
- Yoon BE & Lee CJ (2014). GABA as a rising gliotransmitter. *Front Neural Circuits* **8**, 141.
- Yu J, Proddutur A, Elgammal FS, Ito T & Santhakumar V (2013). Status epilepticus enhances tonic GABA currents and depolarizes GABA reversal potential in dentate fast-spiking basket cells. *J Neurophysiol* **109**, 1746–1763.
- Zucker RS & Regehr WG (2002). Short-term synaptic plasticity. *Annu Rev Physiol* **64**, 355–405.

Additional information

Competing interests

The authors declare no competing financial interests.

Author contributions

A.U.F.: experimental design and project conception, electrophysiology, calcium imaging and immunofluorescence experiments, analysis and interpretation of data, writing of manuscript; N.I.C.M.: experimental design, electrophysiology, analysis and interpretation of data, writing of manuscript; T.D. and D.D.T.: laser microdissection, RNA sequencing; J.O.F.: electrophysiology, analysis of data; D.G.: experimental design and project conception, interpretation of data; K.K., A.M. and J.W.: experimental design, RNA sequencing, analysis and interpretation of data; V.R.: immunofluorescence, analysis and interpretation of data; M.A.X.-F.: experimental design, calcium imaging, interpretation of data, manuscript writing; E.F.: experimental design and project conception, interpretation of data, manuscript writing. All authors have read and approved the final version of this manuscript and agree to be accountable for all aspects of the work in ensuring that questions related to the accuracy or integrity of any part of the work are appropriately investigated and resolved. All persons designated as authors qualify for authorship, and all those who qualify for authorship are listed.

Funding

This work was supported by the Priority Program 1608 'Ultrafast and temporally precise information processing: normal and dysfunctional hearing' of the Deutsche Forschungsgemeinschaft (grant Fr 1784/17-1 to E.F.) and the Research Initiative Membrane Biology RIMB (to D.G. and E.F.). Further support was provided by the Erasmus Mundus Program Auditory Cognitive Neuroscience CAN (to A.U.F.) and by the Center for Cognitive Science, a research initiative of the Federal State of Rhineland–Palatine.

Acknowledgements

We thank Jennifer Winkelhoff, Ralph Reiss and Tina Kehrwald for excellent technical assistance, Erik Frotscher for input on miniature synaptic events, and Lucille A. Moore for valuable tips concerning pentobarbital. We are grateful to Dr Jochen W. Deitmer, who provided access to the confocal microscope. Finally, we thank Elisa G. Krächan and Dr Jan J. Hirtz for helpful comments on the manuscript.